

Changes in drought characteristics in Earth system model simulations of the past and future

By

Kemisola Esther Adeniyi
3118997

Supervised by

Prof. Dr. Veronika Eyring

Prof. Dr. Markus Reichstein

Department of Climate Modelling

University of Bremen

14. November.2019



Table of contents

Table of contents.....	i
Table of figures.....	ii
ABSTRACT.....	iii
1. INTRODUCTION.....	1
2. MOTIVATION AND AIM OF THE THESIS.....	3
3. SCIENTIFIC BACKGROUND.....	4
3.1. THE HYDROLOGIC CYCLE.....	5
3.2 DROUGHT INDICATORS.....	5
4. METHODOLOGY.....	7
4.1. STANDARD PRECIPITATION INDEX.....	8
4.2. STANDARD PRECIPITATION EVAPORATION INDEX.....	10
4.2.1. THORTHWAITE EQUATION.....	11
4.2.2. PENMAN MONTEITH EQUATION.....	12
4.2.3. HARGREAVES EQUATION.....	13
5. TOOLS AND DATA.....	16
5.1. ESMValTool.....	16
5.2. OBSERVATIONAL DATASET.....	17
5.3. CLIMATE MODELS: CMIP ENSEMBLE.....	17
6. RESULTS AND DISCUSSION.....	20
6.1. SELECTION OF PET CALCULATION METHOD.....	20
6.2. HISTORICAL CHANGES IN DROUGHT INDICES.....	25
6.3. HISTORICAL AND FUTURE CHANGES IN DROUGHT CHARACTERISTICS.....	31
7. SUMMARY AND OUTLOOK.....	35
REFERENCES.....	37
APPENDIX.....	43

Table of figures

Figure 1-1: Sequence of drought impacts with time [Kan et al., 2017].	3
Figure 3-1: The global water cycle, from National Weather Service [NOAA].	6
Figure 6-1: Multi-model mean (3 CMIP6 models) percentage difference between the future (2050-2100) and historical (1950 to 2000) simulations, showing average SPEI (top left), number (top right), duration (bottom left) and severity index (bottom right) calculated based on SPEI-TH. Produced using the ESMValTool, version 2.0a1, recipe_drought_events.yml.	22
Figure 6-2: Same as Figure 6-1 but calculated based on SPEI-Hg. Produced using the ESMValTool, version 2.0a1, recipe_drought_events.yml.	22
Figure 6-3: Same as Figure 6-1 but calculated based on SPEI-PM. Produced using the ESMValTool, version 2.0a1, recipe_drought_events.yml.	23
Figure 6-4: Same as Figure 6-1 but calculated based on the internal PET variable from the individual models. Produced using the ESMValTool, version 2.0a1, recipe_drought_events.yml.	23
Figure 6-5: Histogram plot of SPI from the ERA-Interim observation (black) and the historical simulations from 7 CMIP6 models (colours) between 1979 and 2014 [upper panel] and their difference [lower panel]. (Produced using the ESMValTool, version 2.0a1, recipe_spikeah_histogram.yml)	26
Figure 6-6: Histogram plot of SPEI-PM from the ERA-Interim observation (black) and the historical simulations from 7 different CMIP6 models (colours) between 1979 and 2014 [upper panel] and their difference [lower panel]. (Produced using the ESMValTool, version 2.0a1, recipe_spei_histogram_area.yml)	26
Figure 6-8: Percentage difference between multi-model mean of CRU observations (1979 to 2014) and 7 CMIP6 models historic simulations (1979 to 2014) showing average SPI/SPEI, number, duration and severity index of drought events using the SPI. Produced using the ESMValTool, version 2.0a1, recipe_drought_events.yml.	30
Figure 6-10: Histogram showing the historical (1950 - 2000) and future (2050 - 2100) simulations from 7 CMIP6 models using SPEI-PM. Produced using the ESMValTool, version 2.0a1, recipe_spei_PM_histogram_area.yml.	31
Figure 6-11: Percentage difference of 7 CMIP6 models showing average SPI/SPEI, frequency, duration and severity of drought events using SPI (left) and SPEI-PM (right) between the historic (1950 to 2100) and SSP5-85 (2050-2100) multi-model mean. Produced using the ESMValTool, version 2.0a1, recipe_drought_events.yml.	34

List of Tables

Table 4-1.: Classification of drought and pluvial categories with corresponding SPI/SPEI values and the probability of each event [Varouchakis and Corzo, 2019].	9
Table 4-2: Features, advantages and disadvantages of the various indices [Lloyd-Hughes and Saunders, 2002; Vicente-Serrano et al., 2010; W.M, 1984; World Meteorological Organisation, 2012].	15
Table 5-3: CMIP6 models used in this analysis; Adapted from: [Studies, 2018; Swart et al., 2019; Tatebe and Watanabe, 2018; Wu et al., 2018; Yukimoto et al., 2019]	19

ABSTRACT

The goal of this Master thesis is to evaluate the representation of drought events in historical simulations carried out with the new generation of Earth system models (ESMs) participating in the Coupled Model Intercomparison Project Phase 6 (CMIP6), and to characterize how frequency, intensity and duration of droughts are changing in the future under a specific forcing scenario (here SSP5-8.5). Results from different drought indices, in particular the Standardized Precipitation Index (SPI) that is based on precipitation only and the Standardized Precipitation Evapotranspiration Index (SPEI) are compared. For SPEI, different methods for calculating potential evapotranspiration (PET) have been proposed in the literature following the equations of Thornthwaite (SPEI-Th), Hargreaves (SPEI-Hg), and Penman Monteith (SPEI-PM). These methods approximate PET with increasing complexity and number of variables: SPEI-Th is based on temperature only, SPEI-Hg uses monthly mean daily minimum and maximum temperature and SPEI-PM is additionally taking into account cloud cover, air pressure and wind speed. Due to the lack of available output variables and the verification of all SPEI methods for the historical period, for the analysis of ESMs often the methods based on empirical correlations between temperature and PET have been applied. However, using output from three CMIP6 ESMs that provided all variables required for the calculation of all three SPEI methods plus the internally simulated PET variable, this thesis in a first step shows that only the SPEI-PM method is able to correctly reproduce drought characteristics similar to the results achieved if the model's PET variable is used. While SPEI-PM projects a moderate increase in extreme drought events especially in the subtropics, SPEI-Th projects an unrealistic drastic increase in the frequency and duration of droughts nearly globally and SPEI-Hg a strong increase in subtropical regions and the mid-latitudes, both inconsistent with calculations based on the models' PET variable. In a second step, a larger ensemble of seven CMIP6 models is therefore only analyzed with the SPI and SPEI-PM indices. Except for certain regions, SPI and SPEI-PM drought characteristics calculated from the multi-model mean in comparison to ERA-Interim and the Climate Research Unit (CRU) dataset for the period 1979 to 2014 only show small deviations. Percentage changes in drought characteristics between the future (2050-2100) and the historical (1950-2000) period for SPI and SPEI-PM show in general good agreement, although SPEI-PM results in larger changes in drought frequency compared to SPI. SPEI-PM shows an increase in frequency and

severity of drought events in the already dry subtropics by over 200% and 50% while SPI shows an increase in same characteristics by over 150% and 30%, respectively.

1. INTRODUCTION

The Intergovernmental Panel on Climate Change (IPCC) Fifth Assessment Report (AR5) stated that the type, frequency and intensity of extreme events are expected to change with climate warming [IPCC, 2014a]. In the past century, the average global mean surface temperature has increased by about 1.5°C [IPCC, 2018]. This change in climate can increase the frequency of natural processes, some of which are hazardous to humans and the ecosystem at large. Droughts are one of these natural hazardous phenomena [Hagman *et al.*, 1984]. They are extreme climate events that occur as a result of very little or no precipitation. Severe drought events which have been observed in the last decades include the 2005 and 2010 Amazon droughts (characterized as “100 year events” [Lewis *et al.*, 2011; Marengo *et al.*, 2008], the 2009–2011 drought in China [Barriopedro *et al.*, 2012; Sun and Yang, 2012], the Horn of Africa drought between 2010 and 2011 [Lyon, 2014; Masih *et al.*, 2014], the Texas drought in 2011 [Nielsen-Gammon, 2012], and the California drought [AghaKouchak *et al.*, 2014; Cheng *et al.*, 2016] between 2012 and 2015 to mention a few.

In an IPCC Special Report on Managing the Risks of Extreme Events and Disasters to Advance Climate Change Adaptation [IPCC, 2012], the increase in extreme events (e.g. droughts) are categorized as one of the major challenges occurring with a changing climate. In general terms, a drought is a “prolonged absence or marked deficiency of precipitation, that results in water shortage for a community or group of people” or a “period of abnormally dry weather, prolonged enough as a result of lack of precipitation to cause an extreme hydrological imbalance” [IPCC, 2012]. This eventually leads to a persistent lack of water resources, resulting in dying crops and shortage of other agricultural products becoming an economic problem. Droughts are usually regional in extent and since different regions have different climatic characteristics, a drought in Brazil will be different from a drought in Asia or Africa in terms of intensity, duration, frequency and spatial coverage.

Droughts as an event are very complex and difficult to define, as a result of the multiple mechanisms causing them [Kiem *et al.*, 2016]. It can be considered as a creeping phenomenon [Tannehill, 1947] hence the need for it to be carefully monitored. Climatic phenomena such as monsoons and El Nino Southern Oscillation (ENSO) can affect changes in drought occurrence in some regions [Hilario *et al.*, 2009; Lyon *et al.*, 2006]. Changes in droughts and assessments of their trends depend on the type of drought, the model assumptions and datasets [Sippel *et al.*,

2018]. Droughts are usually not defined based on absolute thresholds only, but rather as an anomalous condition with precipitation being the primary factor controlling its formation. Additionally, other factors such as temperature, wind-speed, radiation, and soil moisture are important variables. The definition of a water deficit (drought) is a complex function of water availability and its use. The time scales over which precipitation deficits accumulate become very crucial and classify droughts into different types or categories. According to the IPCC Fifth Assessment Report of Working Group [IPCC, 2012], droughts can be grouped into different types (see also Figure 1-1):

- (i) Meteorological drought: defined as deficit of precipitation.
- (ii) Agricultural drought: takes place when soil moisture is inadequate, thereby resulting in a lack of crop growth and production. This can be referred to as a short term drought.
- (iii) Hydrological drought: takes place when an agricultural drought has occurred for an extensive period of time over a large region, thereby causing shortages of water resources and resulting into negative anomalies in groundwater, reservoirs and stream levels.

Figure 1-1 below illustrates how the natural climate changes with time, thereby resulting into different categories of droughts and their areas of impact on the community and the world inhabitants.

Martin [2018] summarized that several studies consistently show an increase in drought frequency both in observations and in climate model projections in particular for the most extreme droughts in subtropical region. However, quantitative differences exist when different indices are used to identify and project droughts [*Mishra and Singh*, 2010]. *I H Taylor et al.* [2013] classified four major sources of uncertainty based on: climate model, future scenario, drought index, and drought threshold uncertainties. They concluded that the drought index selection is the most important factor affecting the uncertainty in future drought projections [*I H Taylor et al.*, 2013].

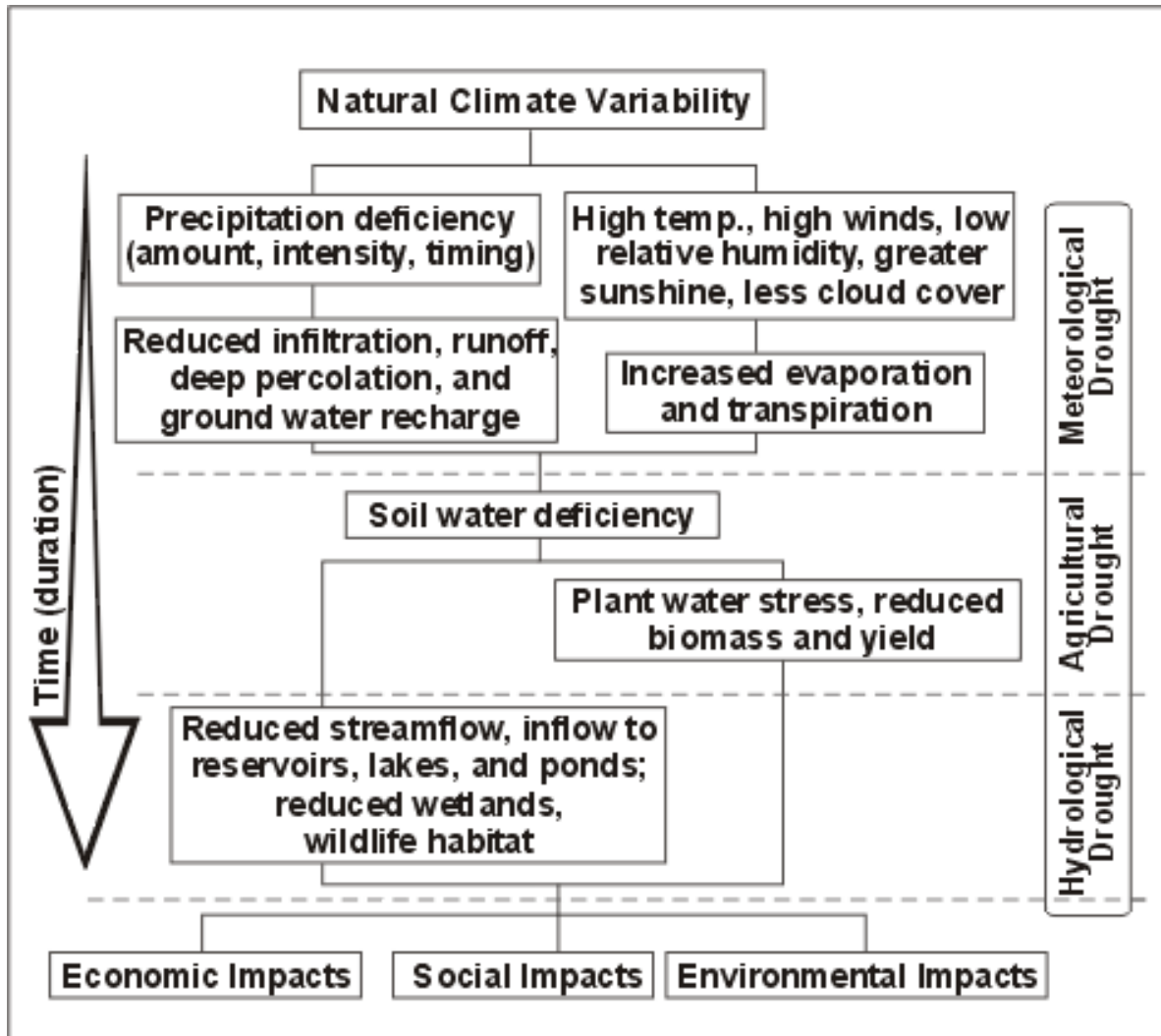


Figure 3-1: Sequence of drought impacts with time [Kan et al., 2017].

2. MOTIVATION AND AIM OF THE THESIS

The goal of the Master thesis is to quantify and characterize the historical and future evolution of meteorological drought characteristics in CMIP6 model simulations. In particular, the SPI and the Standardized Precipitation Evaporation Index (SPEI). Drought characteristics (average SPI/SPEI, frequency, duration and severity of drought events) are analyzed using historical simulations and future climate projections from the CMIP6 ensemble [Eyring et al., 2016a] together with meteorological reanalysis from ERA-Interim [Dee et al., 2011].

The SPEI takes the potential evapotranspiration (PET) as an additional variable for characterizing drought events. Potential evapotranspiration is the amount of evaporation that will

take place through evapotranspiration if sufficient water source were available. A couple of limitations are however known for the (PET) calculation [Greve *et al.*, 2014] in SPEI. A first aim of the thesis is therefore to compare results from PET calculations based on the temperature-based Thornthwaite equation with other approaches which include the Hargreaves equation [Hargreaves George and Allen, 2003] and the Penman Monteith equation [Shaw and Riha, 2011]. These equations (see Section 4.2.2 and 4.2.3) use multiple variables and are expected to better account for changes in drought characteristics. A detailed study of data from ERA-Interim, as well as both historical and future simulations from CMIP6 models is presented on a global scale and the results are compared in order to ascertain the best drought index for the identification of meteorological droughts.

Chapter 3 provides a brief review of the scientific background for this thesis for the relationship between the hydrologic cycle and droughts (Section 3.1) and drought indicators (Section 3.2). Chapter 4 focuses on the methods that are used in this thesis for the calculation of drought indices, their mathematical formulations and approaches. The observational datasets and the available CMIP6 models used for the evaluation of historical and for future projections of droughts, as well as the description of the program code that has been built into the Earth system model evaluation tool (ESMValTool, Eyring *et al.*, 2016b) as part of this thesis are described in Chapter 5. The results of the thesis are discussed in Chapter 6. Chapter 7 closes with a summary and outlook.

3. SCIENTIFIC BACKGROUND

The IPCC AR5 concluded that the warming of the climate system is unequivocal [IPCC, 2014b]. It has been anticipated that direct impact of climate change on water resources will be mainly through evapotranspiration. Hydrological changes constitute one of the most significant potential impacts on the global scale [IPCC, 2014b]. According to GCMs, this will have a significant impact on the hydrologic cycle and eventually on the nature of drought in the future. This is because water deficit propagates through the subsurface part of the hydrological cycle and result into different types of droughts [Wilhite, 2000]. Although the characteristics of droughts (i.e. the frequency, duration and severity) changes as it propagates through the subsurface, but not all meteorological droughts develop into hydrological droughts.

3.1. THE HYDROLOGIC CYCLE

The hydrologic cycle (Fig. 3-1) is the continuous movement of water between the oceans, land, and atmosphere. The hydrologic cycle can be explained beginning with the evaporation of water from the ocean surface, as the atmosphere continues to warm, moist air is lifted and the air present tends to hold more moisture, thereby causing more water to be evaporated. As the lifted moist air cools, the water vapor in it condenses to form clouds. This moisture in the cloud is transported around the globe and eventually returns as precipitation. Precipitated water can evaporate again or penetrate into the surface and become groundwater. Groundwater either seeps its way into other water bodies or released back into the atmosphere through transpiration. The rest of the water that remains on the earth surface is considered as run off which later finds its way into rivers and carried back into the oceans where the cycle begins again. The movement of the moisture around the globe with increasing temperatures due to climate change sometimes lead to an increase in heavy rain events thereby resulting into frequent flooding. On the contrary, more evaporation with hotter temperatures will dry out the soils and increase water demand, hence, leading to frequent and intense drought. The water deficit propagates through the subsurface part of the water cycle and leads into the formation of various kinds of droughts [Peters, 2003; Wilhite, 2000]. In other words, in a warming climate, an accelerated hydrologic cycle will result into more severe droughts, but at the same time will include periods of intense flooding, thereby exposing agricultural and economic systems to an unstable state.

3.2 DROUGHT INDICATORS

Drought indicators are considered as variables used to describe the drought condition. This include precipitation, temperature, streamflow, soil moisture and so on [Fuchs, 2016]. While drought indices are typically computed numerical representations of drought severity, usually assessed using the climatic or hydro-meteorological inputs such as the indicators listed above. They measure the state of droughts at a particular period of time qualitatively.

Large uncertainties still exist with regard to the land-atmosphere feedback related to drought [Orlowsky and Seneviratne, 2012]. Large uncertainties also exist in the projection of droughts in the future. *I H Taylor et al.* [2013] classified four major sources of uncertainty based on: climate model, future scenario, drought index, and drought threshold uncertainties. They concluded that

the drought index selection is the most important factor affecting the uncertainty in future drought projections [I H Taylor et al., 2013]. Burke and Brown [2008] used four different drought indices to assess the uncertainty in future drought projections: the Standard Precipitation Index (SPI), the precipitation and potential evapotranspiration anomaly (PPEA), the Palmer drought severity index (PDSI), and the Soil Moisture Anomaly index [Smakhtin and Schipper, 2008]. They concluded that indices that include some measure of the atmospheric demand for moisture, that is, the PPEA and PDSI projects an increase in the proportion of the global land surface changes in drought, ranging from an additional 5–45%. While SPI, based only on precipitation, projected a much smaller global changes ranging from 5% less to 10% more of the land surface [Burke and Brown, 2008].

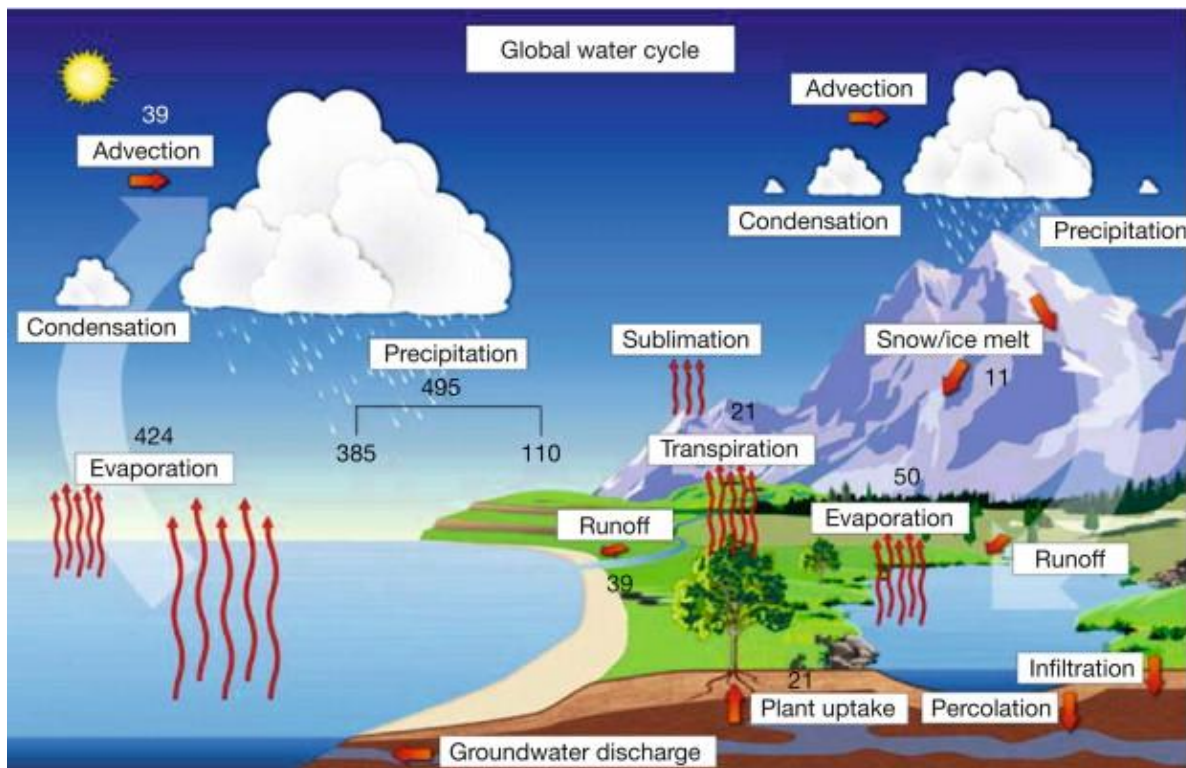


Figure 3-1: The global water cycle, from National Weather Service [NOAA].

Depending on the drought type and index, changes of drought conditions in observation-based datasets and future projections by Global Climate Models (GCMs) [Orlowsky and Seneviratne, 2012] differ substantially [Burke and Brown, 2008; I H Taylor et al., 2012a]. Recent studies [Dai, 2012; Sheffield et al., 2012] on observed global drought changes over the 20th century also find contradictory results, depending on the drought index applied. A number of investigations have analyzed droughts considering future climate change [Li et al., 2009; Sanjairaj et al., 2012;

Strzeppek et al., 2010]. Much of the reported research has analyzed drought indices using GCM and Regional Climate Models [*Dubrovský et al.*, 2009; *Mishra and Singh*, 2010; *Mishra et al.*, 2009; *Mpelasoka et al.*, 2008], they all confirmed worsening drought conditions in the future for some regions.

In the context of climate projections, previous scientific research suggests that changes in simulated soil moisture drought are mostly driven by changes in precipitation, with increased evapotranspiration from higher vapor pressure deficit often linked to increased temperature and Earth radiation modulating some of these changes [*Orlowsky and Seneviratne*, 2012; *Sheffield and Wood*, 2008]. It should however be considered that under strong drought conditions, soil moisture becomes limiting for evapotranspiration, which further limits soil moisture depletion. The choice of variables (e.g. precipitation, soil moisture), drought time scale and respective time series can define or determine the ranking or analysis of drought events [*Vidal et al.*, 2010].

4. METHODOLOGY

This section introduces different indices that can be used for the detection and analysis of drought events, with focus on comparing their frequency, duration and severity. These include the SPI and the SPEI (using the Thornthwaite (SPEI-Th), Penman Monteith (SPEI-PM) and Hargreaves (SPEI-Hg) method). The analysis of these indices is implemented in new recipes and diagnostics of the ESMValTool [*Eyring et al.*, 2016b], a community diagnostics and performance metrics tool for the evaluation of Earth System Models (ESMs). It allows for routine comparison of single or multiple models, either against predecessor versions or against observations.

There is currently no particular index capable of adequately characterizing drought conditions for every place and every time period [*Svoboda et al.*, 2015]. Hence the selection of the drought index is based on drought type, objective and information available to drought users [*Smakhtin and Schipper*, 2008]. It is crucial to establish a comparison between the SPI and the SPEI in order to determine if the inclusion of the PET [*Greve et al.*, 2014] parameter produces significantly different index values. *Stagge* [2014] confirmed that inclusion of PET makes a large difference in the drought index especially during the summer, because the PET occupies a greater portion of the climatic water balance during this time.

The SPI and SPEI are described in Sections 4.1 and 4.2 respectively. An overview of the variables, advantages and disadvantages of the indices is presented in Table 4-1.

4.1. STANDARD PRECIPITATION INDEX

The most commonly used index for detecting meteorological droughts is the SPI. The SPI describes the probability of occurrence of rainfall when compared to the actual supposed rainfall climatology of a certain geographical location over a long period of time [Guenang and Francois, 2014]. This index was developed by McKee [1993], who described that some of the major factors that are important in any analysis of a drought are its time scale, the expected frequency of an event and its precipitation deficit. Frequency, duration and intensity of droughts are the functions and parameters that depend on the explicitly established time scales.

The calculation of SPI for a certain time scale needs monthly mean precipitation data [Hayes *et al.*, 2011]. SPI is simple to calculate as it requires only precipitation as input parameter and can be compared across regions of different climatic zones. Other conditions related to drought such as temperature, evapotranspiration, wind speed or soil capacity are not considered in this index. SPI can be computed for different time scales (1-month SPI, 3-month SPI, 6-month SPI up until 24-month SPI). According to the SPI user guide compiled by Svoboda *et al.* [2012], a 3-month SPI indicates short and medium-term moisture conditions and provides a seasonal estimation of precipitation, a 6-month SPI indicates seasonal to medium-term trends in precipitation and is recommended to be more sensitive, a 9-month SPI indicates an inter-seasonal precipitation patterns over a medium timescale duration while 12-month to 24-month timescales are the cumulative result of shorter periods that may be above or below normal. In this thesis paper, the 6-month SPI time scale analogous to Martin [2018] is used, which is calculated with the SPEI R package [Begueria *et al.*, 2014] that was available in the ESMValTool. The fact that SPI can be computed on multiple timescales allows for temporal flexibility in the evaluation of precipitation conditions relative to the water supply. Accumulated values of the SPI can be used to analyze the severity of droughts. Ideally, one needs at least 20-30 years of monthly values, with 50-60 years (or more) being optimal and preferred [Guttman, 1994]. The program can still run with missing data, but it will affect the confidence of the results, based on the distribution of the missing data in relation to the length of the record.

The first step in the calculation of the SPI is to determine the probability density function (usually a Gaussian function is used). The full computation is quite complicated, *Guenang and Francois* [2014] can be referred to for details. This computation describes the long-term behavior of the data, but usually, monthly precipitation is not normally distributed, hence a transformation is performed such that the derived SPI values follow a normal distribution. The number of standard deviations that the observed value would deviate from the long-term mean, for a normally distributed random variable is referred to as the SPI. A fit to the cumulative precipitation usually a gamma distribution is applied to calculate the SPI. [*Lloyd-Hughes and A. Saunders, 2002; Martin, 2018*].

From the SPI, the severity index based on *Peters* [2014] is calculated. The index is given by:

$$(Eq. 1) \quad SI = \frac{\sum_{i=1}^n SPI * T_{event}}{SPI * \bar{T}}$$

Where SPI is the monthly SPI during the event, T_{event} is the number of months in which the SPI exceeds the standard threshold, \overline{SPI} is the mean value of all the months in which SPI exceeds the threshold, and \bar{T} is the mean duration of all the events that exceed the threshold.

Negative SPI values are rainfall deficits, whereas positive SPI values are rainfall surpluses. The intensity of drought events can then be classified according to the magnitude of negative SPI. For instance, negative SPI values lower than -2 are often regarded as extreme drought conditions. This classification can be used for risk management and assessment. Table 3-1 classifies drought categories with respect to its SPI threshold and the probability of each event.

Table 4-1.: Classification of drought and pluvial categories with corresponding SPI/SPEI values and the probability of each event [Varouchakis and Corzo, 2019].

Drought Category	SPI/SPEI Value	Probability of events(%)
Extreme dry	SPI/SPEI >= -2.0	2.3
Severe dry	-2.0 <= SPI/SPEI < -1.5	4.4
Moderate dry	-1.5 <= SPI/SPEI < -1.0	9.2
Neutral/Normal	-1.0 <=SPI/SPEI < 1.0	68.2
Moderate wet	1.0 <= SPI/SPEI < 1.5	9.2
Severe wet	1.5 <= SPI/SPEI < 2.0	4.4
Extreme wet	SPI/SPEI >= 2.0	2.3

4.2. STANDARD PRECIPITATION EVAPORATION INDEX

The SPEI is an extension of the SPI. It was originally proposed by *Vicente-Serrano et al.* [2009] as an improved and effective drought index to study the effect of global warming on drought severity. A complete description of the theory and other computational details behind the SPEI was also explained in comparisons with the PDSI and the SPI [*Vicente-Serrano et al.*, 2009]. The SPEI takes monthly precipitation and PET into account. The same categorization and probability for dry and wet events for SPI is also applicable for SPEI and shown in Table 4-1.

The SPEI was described to be an important and useful index for comparing and analyzing meteorological droughts. Recent studies show that SPEI should be calculated using methods different from the Thornthwaite equation which approximated the PET based only on the monthly mean temperature [*Chen et al.*, 2005; *Nikam et al.*, 2014]. In this Master thesis, the Thornthwaite equation, Penman Monteith equation, and Hargreaves will be looked into to establish the importance of PET and the difference between these methods.

Evaporation is defined as the net loss of moisture from a wet surface, resulting from a phase change of liquid to vapour based on the weather parameters. Transpiration is the process by which moisture is conveyed through plants from roots to small pores (stomata) where it changes to vapour and released into the atmosphere. Evapotranspiration is the sum of evaporation and plant transpiration from the earth surface to the atmosphere.

Potential evapotranspiration is therefore the amount of evaporation that will take place through evapotranspiration if sufficient water source or soil moisture were available. It is one of the fundamental processes controlling the hydrological and energetic equilibrium of our planet, and its knowledge is crucial for climatic and drought studies. Evaporation and transpiration takes place simultaneously and both processes depend on solar radiation, air temperature, relative humidity and wind speed. PET is very much different from the actual evapotranspiration. The actual evapotranspiration is the quantity of water that is actually removed from a surface due to the processes of evaporation and transpiration [*Hubbart and Pidwirny*, 2010]. Consequently, it constitutes one of the major phenomena in the hydrological budget, especially in arid and semi-arid regions.

The difference (water surplus or deficit) between precipitation and PET, can be aggregated at different time scales and calculated as:

$$(Eq. 2) \quad D_i = P_i - PET_i$$

The SPEI is calculated with the SPEI R package [Begueria et al., 2014] that was available in the ESMValTool at the beginning of this thesis. The Thornthwaite method was already included in this R package, other alternatives to calculating PET, that is the Penman Monteith and Hargreaves were implemented into the R package as the study proceeded. The SPEI can also be calculated on a wide range of time scales usually between 1 to 48 months just like the SPI. In this work a 6-month SPEI using a Log-Logistic distribution is computed.

4.2.1. THORTHWAITE EQUATION

The easiest approximation to calculate the PET for the SPEI is using Thornthwaite equation [Thornthwaite, 1948], which is based on average monthly temperature. It is considered unreliable under a changing climate as it can over-estimate the degree of water deficit [Shaw and Riha, 2011]. The relationship between monthly means of daily averaged temperatures and Potential evapotranspiration is given by [Thornthwaite, 1948]:

$$(Eq. 2) \quad PET = 16 \left(\frac{L}{12}\right) \left(\frac{N}{30}\right) \left(\frac{10T_d}{I}\right)^\alpha$$

Where

PET = estimated potential evapotranspiration

Td = daily average temperature

N = Number of days in a month

L = average hours of the month

$$\alpha = (6.75 * 10^{-7})I^3 - (7.71 * 10^{-5})I^2 + (1.72 * 10^{-2})I + 0.49239$$

$$I = \sum_{i=1}^{12} \left(\frac{T_{m_i}}{5}\right)^{1.514} \text{ is the annual heat index}$$

4.2.2. PENMAN MONTEITH EQUATION

Using the temperature based Thornthwaite equation for calculating PET may no longer be suitable under a changing climate. *Shaw and Riha* [2011] introduced other model equations based on more variables, that is the Penman Monteith (PM) equation. In 1948, Penman combined the energy balance with the mass transfer method and derived an equation to compute the evaporation from an open water surface from standard climatological records of radiation, temperature, humidity and wind speed [*Penman and Keen*, 1948]. The PM equation is considered the most physically correct model based on the fact that it has a solid theoretical basis and a dependency on all relevant meteorological factors, which include wind-speed, air temperature, net radiation, air humidity and vapor pressure. The PM equation was also calculated using the SPEI R package [*Beguiria et al.*, 2014] which was built into the ESMValTool in the process of this thesis.

Several empirical methods have been developed over the years to estimate evapotranspiration from different climatic variables based on the combination of an energy balance and an aerodynamic formula. *Shaw and Riha* [2011] discussed the two equations as PET estimators and described PM as a widely used and most suitable method because it additionally considers influences of vegetation and aerodynamic properties. An updated PM equation was recommended by Foods and Agricultural Organization (FAO)-56 [*Allen et al.*, 1998] given as:

$$(Eq. 3) \quad \lambda E_T = \frac{\Delta(R_n - G) + P_a C_p \left(\frac{e_s - e_a}{r_a} \right)}{\Delta + \gamma \left(1 + \frac{r_s}{r_a} \right)}$$

Where R_n = net radiation

G = soil heat flux

$e_s - e_a$ = vapour pressure deficit of air

r_a = mean air density at constant pressure

C_p = specific heat of air

D = slope of saturation vapour pressure

γ = Psychometric constant

r_s = bulk surface resistance

r_a = aerodynamic resistance

Some of the meteorological data (expressed in several units) required for PM equation can be directly measured in weather stations. Other parameters are related to commonly measured data and can be derived with the help of a direct or empirical relationship. The computation of all data required for the calculation of the reference evapotranspiration by means of the FAO PM method can be referred to according to *Zotarelli* [2013]. Appropriate procedures for estimating missing data are also provided. Due to this, the SPEI R package [*Begueria et al.*, 2014] contains several implementations of PM depending on the available variables. For this thesis, precipitation, cloud cover, wind speed, pressure, minimum and maximum temperature are used (see Table 4-2).

4.2.3. HARGREAVES EQUATION

There are several versions of Hargreaves equation. In 1975, Hargreaves published the Hargreaves equation, which is referred to as a semi-empirical approximation. It introduces extra-terrestrial radiation in combination with temperature as indicators of global radiation while the daily temperature ranges as an indicator of cloudiness [*Hargreaves George and Allen*, 2003]. Cloudiness is inversely related to temperature range and the influence of relative humidity is also related to this relationship. The introduction of temperature range into the equation compensates for the influence of advection as it depends on the interaction between temperature, wind speed, humidity and air pressure.

According to *Hargreaves George and Allen* [2003], Hargreaves equation is said to be published in 1975 as

$$(Eq. 6) \quad ET_0 = 0.0135R_s (TC + 17.8)$$

Hargreaves George and Samani [1982] proposed the predictive form of the equation as

$$(Eq. 7) \quad R_s = K_{RS} R_a TR^{0.5}$$

Where R_s is the global solar radiation at the surface, K_{RS} is the empirical coefficient, R_a is the extraterrestrial radiation of the crop surface and TR is the temperature range that is (Tmax-

Tmin); where Tmax is the mean daily maximum temperature and Tmin is the mean daily minimum temperature. Generally, values of K_{RS} is known to slightly increase with temperature.

Hargreaves [1983] found a value of 0.16 using climatic data from the Senegal River Basin. Combining equation 3 and 6 using K_{RS} as 0.16 [*Hargreaves George and Samani*, 1982].

G L Hargreaves et al. [1985] derived the equation

(Eq. 8)
$$ET_0 = 0.0022R_a (TC + 17.8TR^{0.50})$$

This equation was adopted in FAO-56 by *Allen et al.* [1998] for predicting R_s when data are missing. The equation was later improved in 1985. *G L Hargreaves et al.* [1985] recommended that the coefficient be increased to 0.0023. This adjustment resulted in the so-called 1985 Hargreaves equation

(Eq. 9)
$$ET_0 = 0.0023R_a (TC + 17.8TR^{0.50})$$

The equation compensates for the absence of R_s and humidity in PM equation. According to the SPEI Package, Hargreaves computes the monthly reference evapotranspiration (ET_0) of a grass crop based on the original Hargreaves equation. For this study, a modified form according to [*Droogers and Allen*, 2002] will be implemented, this is because ERA-Interim observation data does not provide R_s .

Table 4-2: Features, advantages and disadvantages of the various indices [Lloyd-Hughes and Saunders, 2002; Vicente-Serrano et al., 2010; W.M, 1984; World Meteorological Organisation, 2012].

DROUGHT INDEX	VARIABLES REQUIRED	ADVANTAGES	DISADVANTAGES
SPI	Precipitation	<ul style="list-style-type: none"> -It is simple, flexible and can be computed for multiple timescales. -Precipitation data works fine even if incomplete. Data is usually averaged to monthly precipitation. -It is spatially consistent and allows comparisons between different locations and climates. -Its probabilistic nature gives it an historical context which aids decision making. 	<ul style="list-style-type: none"> -It is based only on precipitation. -No use of soil water balance or other variables. Hence, potential evapotranspiration cannot be calculated. -SPI at short time scales (1 to 3 months) when applied to regions of low precipitation could give rise to misleading large positive or negative values.
SPEI-Th	Precipitation PET is calculated based on temperature only	<ul style="list-style-type: none"> -It takes both precipitation and PET as input data -It also allows comparison between locations and climates. 	<ul style="list-style-type: none"> -PET calculation is based only on temperature which makes this method prone to high error.
SPEI-Hg	Precipitation PET is calculated based on the monthly mean of the daily minimum and maximum temperature	<ul style="list-style-type: none"> -It uses less meteorological variables compared to Penman Monteith -It is useful for predicting global solar radiation when data are missing 	<ul style="list-style-type: none"> -It is expected to estimate PET better than SPEI-Th -It require lesser variables in comparison with PM
SPEI-PM	Precipitation PET is calculated based on precipitation, cloud cover, wind speed, pressure, monthly mean of the daily minimum and maximum temperature.	<ul style="list-style-type: none"> -Its use of other meteorological variables makes it a detailed method in identifying drought events and is expected to be the most correct SPEI method. -It is expected to be a better index and method for impacts of droughts in a changing climate under different scenarios. 	<ul style="list-style-type: none"> -Complete data and variables is required which limits its use because of its usual unavailability. - PM is sensitive to vegetation specific parameters, e.g. stomatal resistance or conductance

5. TOOLS AND DATA

5.1. ESMValTool

The ESMValTool is a community development, aimed at diagnosing and understanding biases in models and to provide recommendations for model improvements. It allows for routine comparison of the models, either against different versions or against observations. Its core routines are developed in Python, while diagnostic and plot routines are in addition to python implemented in different languages like NCL, R.

In this thesis, the ESMValTool [Eyring *et al.*, 2016b] is used for the evaluation and analysis of Earth System Models (ESMs). This tool contains a large collection of diagnostics for atmospheric, oceanic and terrestrial variables; not only for the average state, but also for trends, variability and key physical processes. It is used to routinely evaluate different versions of CMIP models with observations.

For this thesis, the existing SPI diagnostic *diag_spi.r* which is called from the *recipe_spei.yml* was used with two modifications to calculate the SPI: following Martin [2018], the time scale was changed from 1 to 6 month and a gamma distribution was used instead of a Pearsons III distribution. The existing *diag_spei.r*, also called from the *recipe_spei.yml* originally as Thornthwaite equation was used with a time scale similar to SPI. The diagnostic scripts call the plot function which produces the plot results as a graphic file (*i.e.*, *png*) and can be seen in the plots produced in this work.

The r scripts (*diag_save_spi_r* and *diag_save_spei_r*) were used to save the SPI and SPEI. They were further evaluated with python scripts (*collect_drought_model.py*) which detect drought events as consecutive number of month with SPI/SPEI < -2 to compute the drought characteristics. Some modifications were done on the diagnostic *diag_save_spei.r* to include SPEI-PM and SPEI-Hg equations with new names called *diag_save_spei_pen.r* and *diag_save_spei_harg.r*. Batch-jobs and recipes that include available CMIP6 models were created for each of these SPEI equations. It also writes out a log file containing the assembled recipe and other information. These recipes are in preparation to be included into version 2 of the ESMValTool assembled into the new *recipe_drought_events.yml*, and the diagnostics into a single script called *diag_newspei.r*. This single script will be expected to run Thornthwaite, Penman Monteith and Hargreaves equation all at once. The additions and modifications to the

drought indices routines that have been done as part of this Master thesis will be contributed to ESMValTool v2.0 and a paper in preparation [Weigel *et al.*, 2019].

5.2. OBSERVATIONAL DATASET

The ERA-Interim reanalysis dataset was used as one dataset in this thesis. ERA-Interim data cover the period from 1979 to present, and uses cycle 31r2 of ECMWF's Integrated Forecast System (IFS) [Dee *et al.*, 2011]. For the comparison of observed and GCM simulated droughts, monthly precipitation data from ERA-Interim, derived from daily precipitation were used for the SPI and SPEI (using additional variables) methods. The ERA-Interim has a spatial resolution of approximately 0.7 degrees by 0.7 degrees with a latitude irregular (Gaussian grid, [Simmons *et al.*, 2006]). The format of both data is in NetCDF.

The Climate Research Unit (CRU) time series for precipitation over land [Harris *et al.*, 2014] with a resolution of 0.5 degrees and data from the time period 1901 to 2001 was used alongside ERA-Interim for the comparison to historical simulations. CRU covers a longer time period than ERA-Interim but includes only precipitation and surface temperature. Therefore, it can be used to compute SPI and SPEI-Th, but not SPEI-Hg and SPEI-PM, which require additional variables.

5.3. CLIMATE MODELS: CMIP ENSEMBLE

Climate models use quantitative methods to simulate the interactions of the atmosphere, oceans, land surface and ice. They are used to study the dynamics of the weather, climate patterns and projections of future climate. These models are created based on certain scenarios which are designed to describe possible future developments of anthropogenic drivers of climate change (i.e., greenhouse gases, chemically reactive gases, aerosols, and land use) for potential socioeconomic developments. They allow an assessment of likely changes in the climate system, impacts on society and ecosystems, and the effectiveness of response options such as adaptation and mitigation under a wide range of future outcomes. [O'Neill *et al.*, 2016].

An expert meeting was setup in 2007, where a process for the development of new community scenarios [Moss *et al.*, 2010] was agreed. The process began with the identification of the Representative Concentration Pathways (RCPs) [van Vuuren *et al.*, 2011], a set of four pathways of land use and emissions of air pollutants and greenhouse gases that spanned a wide range of

possible future outcomes till the end of the twenty first century. The RCPs were the basis for climate model projections in CMIP5 [*E. Taylor et al.*, 2011], and their assessment in the IPCC AR5 [*IPCC*, 2014b]. The Scenario Model Intercomparison Project (ScenarioMIP) is the latest primary activity within CMIP6 which provides multi-model climate projections based on alternative scenarios that are directly relevant to societal concerns regarding climate change mitigation, adaptation and impacts. These climate projections are harnessed by a new set of emissions and land use scenarios. *Riahi et al.* [2011] produced an integrated assessment CMIP6 models [*Eyring et al.*, 2016a] based on new future pathways of societal development, the Shared Socioeconomic Pathways (SSPs) which is closely related to RCPs

In this thesis, 3 models (historical simulation and ScenarioMIP SSP5-85 with r2i1p1f2 ensemble) and another 7 models from the CMIP6 Project (historical simulation and ScenarioMIP SSP5-85 with r1i1p1f1 and r1i1p1f2 ensemble) were used. Model data resolution is bilinearly regridded to the grid of the ERA-Interim and CRU measurements or a common 2 degrees' horizontal resolution for the comparison between model experiments. Monthly data from the CMIP6 historical and ScenarioMIP (SSP5-85) were used. The historical runs with observed GHG forcing starts in 1979 and ends in 2004 for ERA-Interim. For CRU, the historical runs start in 1900 and end in 2016. For comparison between ERA-Interim and CRU, historical run was performed using 1979 to 2004. For CMIP6, the historical runs start in 1850 and end in 2014, for this work, data from 1950 to 2014 is used. The ScenarioMIP experiments start in 2015 and end in 2100. From each GCM, different ensemble run is used (the r1i1p1f1, r1i1p1f2 and r2i1p1f2) where r1 denotes the first run of that GCM, r2 denotes the second run of that GCM, i1 is the first set of initial conditions, p1 is the first setting of physical parameters and f1 is the first set of forcing dataset, f2 is second set of forcing dataset [*Eyring et al.*, 2016a; *K E Taylor et al.*, 2012b], and can only be used if it is available both for the historical and the respective ScenarioMIP experiments, and if it completely covers the 1950–2100 period.

Historical simulations from models participating in CMIP6 [*Eyring et al.*, 2016a] are analyzed in comparison to observations and changes in drought characteristics in the future are assessed under the ScenarioMIP SSP5-85. The historical simulations use as input forcing based on observations including atmospheric CO₂ concentrations, aerosols, and short lived species from

anthropogenic and natural sources. In the ScenarioMIP SSP5-85, atmospheric CO₂ concentration will be more than double by the end of the 21st century compared to 2000 [*Riahi et al., 2011*].

Table 5-3: CMIP6 models used in this analysis; Adapted from: [Studies, 2018; Swart et al., 2019; Tatebe and Watanabe, 2018; Wu et al., 2018; Yukimoto et al., 2019]

Model name	Institute	Resolution	Country	Release Year
BCC-CSM2-MR	BCC	T106, about 110×110 km in the atmosphere, and 30×30 km in the tropical ocean	China	2017
BCC-ESM1	BCC	T106, about 110×110 km in the atmosphere, and 30×30 km in the tropical ocean	China	2017
CanESM5	CCCma	T63 spectral resolution/2.8° and ocean (nominally 1°)	Canada	2019
MIROC6 on Climate	MIROC	T85; 256 x 128 longitude/latitude; 81 levels; top level 0.004 hPa	Japan	2017
MRI-ESM2-0	MRI	T42; 128 x 64 longitude/latitude; 80 levels; top level 0.01 hPa	Japan	2017
NASA/GISS-E2-1-G	NASA-GISS	2.5x2 degree; 144 x 90 longitude/latitude; 40 levels; top level 0.1 hPa	USA	2016
NASA/GISS-E2-1-H	NASA-GISS	2.5x2 degree; 144 x 90 longitude/latitude; 40 levels; top level 0.1 hPa	USA	2016
CNRM-CM6-1	CNRM-CERFACS	Using AOGCM model, 2.5x2 degree; 362 x 294 longitude/latitude; 91 levels; top level 78.4km	France	2017
CNRM-ESM2-1	CNRM-CERFACS	Using ESM model; 2.5x2 degree; 362 x 294 longitude/latitude; 91 levels; top level 78.4km	France	2017
UKESM1-0-LL	MOHC	T85; 192 x 144 longitude/latitude; 85 levels; top level 85km	United Kingdom	2018

6. RESULTS AND DISCUSSION

A subset of the CMIP6 models provided PET (evspsblpot) as an internal variable. These models are CNRM-CM6-1, CNRM-ESM2-1 and UKESM1-0-LL. To select the best approximation to calculate PET, the difference between drought characteristics based on SPEI for future and historical simulations is calculated with this variable and then compared to the result for SPEI calculated using PET based on different approximations (SPEI-Th, SPEI-Hg and SPEI-PM), see Section 6.1.

Based on the result of this first analysis, one PET approximation is selected to calculate SPEI for an extended set of CMIP6 models (BCC-CSM2-MR, BCC-ESM1, CanESM5, MIROC6, MRI-ESM2-0, NASA/GISS-E2-1-G, NASA/GISS-E2-1-H), which do not provide PET as internal variable but all other variables necessary to calculate the drought indices. For these models, the drought characteristics based on SPI and SPEI are compared to ERA-Interim and CRU data for 1979-2014 (Section 6.2). The future changes of drought characteristics are evaluated using the same models, calculating SPI and SPEI on a time series from 1950-2100 combined from historical runs (1850-2014) and projections under the SSP5-85 (2015-2100). Changes are analyzed by calculating differences between the 2050-2100 and 1950-2000 means (Section 6.3).

6.1. SELECTION OF PET CALCULATION METHOD

The common variables used to calculate SPEI are the precipitation and PET. PET can be calculated based on several equations as stated earlier: the Thornthwaite equation, the Hargreaves equation and the Penman Monteith equation. PET calculation following these equations produced different results. To compare the results for these different equations, three CMIP6 models that provided the simulated PET (evspsblpot) as model output variable in addition to the other variables used in the PET calculations were analyzed. The PET which is an aspirational output variable of the Coordinated Regional Climate Downscaling Experiment (CORDEX) [Gutowski Jr et al., 2016] is calculated in different models using different approaches. An example for the calculation of PET in a model (not used in this work) is described by Fita et al. [2019]. One of the major differences between this internal PET variable and other PET approximations used to calculate SPEI is that in the model PET is calculated in

every time step (hours or minutes) and averaged for every month, while for other approximations, PET is estimated from monthly data of other variables.

In any time-series, the neutral conditions defined based on SPI or SPEI occur more frequently than the extreme events, see Table 4.1. Any complete time series contains about 2.3% of extreme dry month [Varouchakis and Corzo, 2019], which can be either sparingly scattered throughout the observed time period or clustered around a certain time. To compare time periods like historical (1950-2000) and future (2050-2100) simulations, it is necessary to calculate the indices for the complete time period (1950-2100) and separate them into partial time series afterwards. In this way, it is possible to get a SPI or SPEI value for every month for 1950-2100, which is based on the same rainfall climatology. This allows to directly compare the partial time series that can then be used to calculate the differences of the number of extreme dry months between the future (2050-2100) and the historical (1950-2000) time period.

These SPI or SPEI values are then used to identify drought events, following *Martin* [2018] who defined a drought event as one or several consecutive months with an SPI of -2 and below. For these events the drought characteristics (average SPI or SPEI, frequency, duration and severity index) were computed for each model individually and thereafter averaged to a multi-model mean. Next, the percentage difference between the multi-model mean of the future and historical simulations is calculated. This is done by dividing the difference between the future and historic simulations by the sum of the two, and thereafter multiplying by 200. Figures 6-1, 6-2, 6-3 and 6-4 show the percentage difference of drought characteristics between the multi-model mean using SPEI-Th, SPEI-Hg, SPEI-PM and SPEI calculated using the internal PET (evspsblpot) variable already available in the respective model.

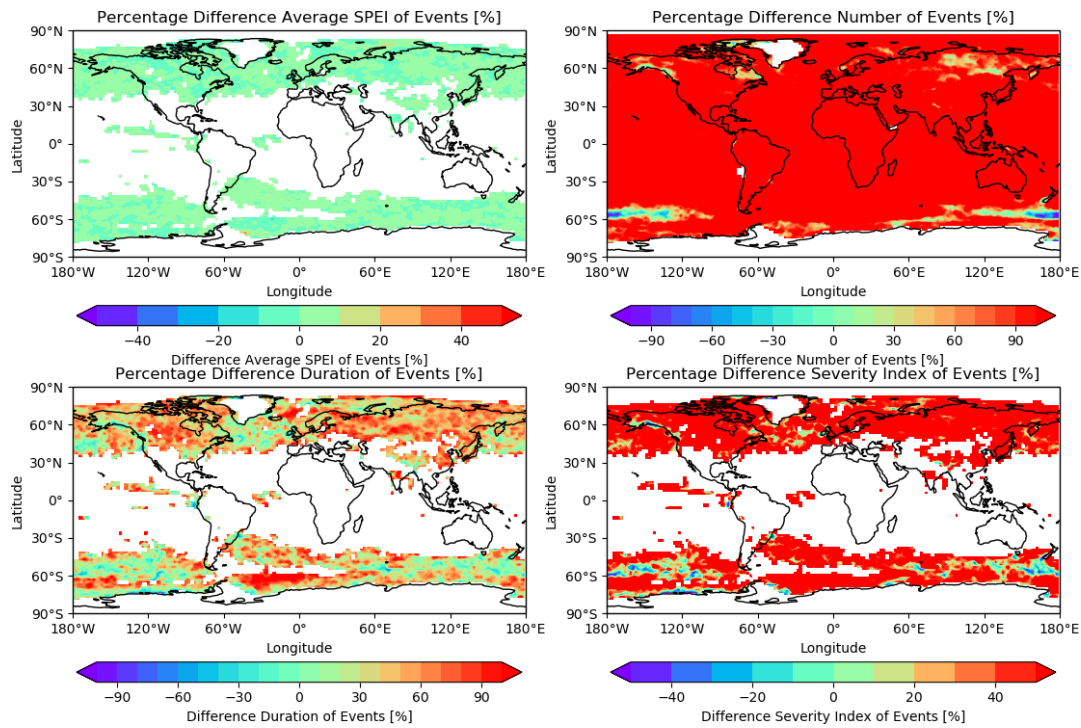


Figure 6-1: Multi-model mean (3 CMIP6 models) percentage difference between the future (2050-2100) and historical (1950 to 2000) simulations, showing average SPEI (top left), number (top right), duration (bottom left) and severity index (bottom right) calculated based on **SPEI-TH**. Produced using the ESMValTool, version 2.0a1, recipe_drought_events.yml.

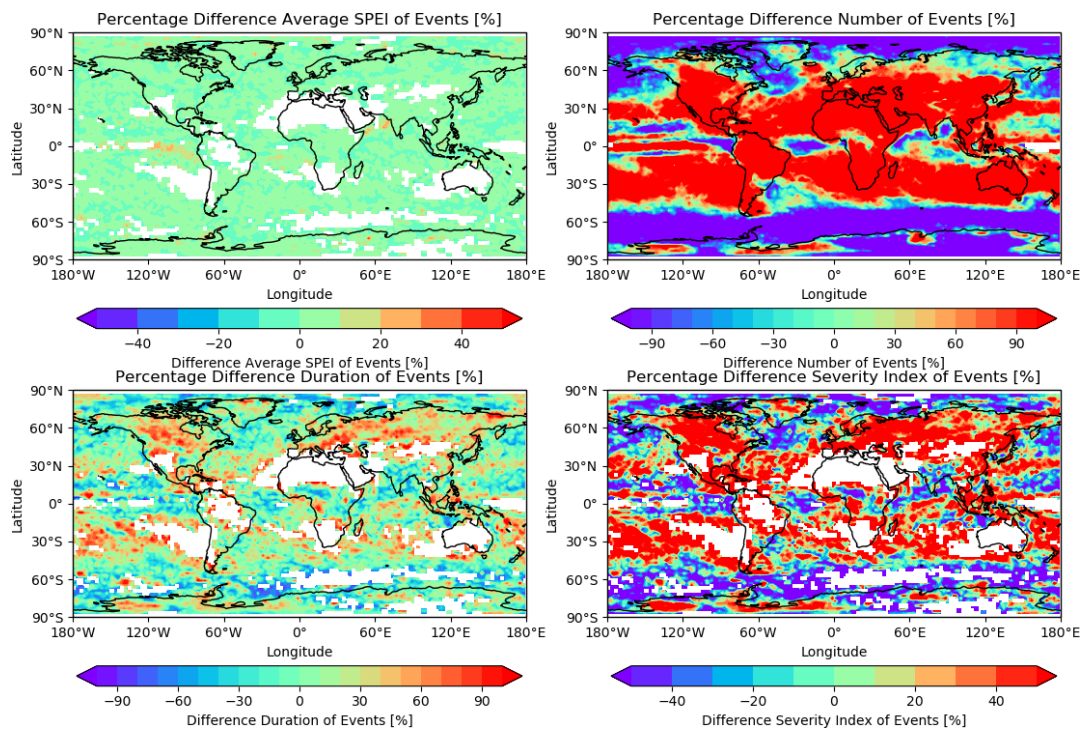


Figure 6-2: Same as Figure 6-1 but calculated based on **SPEI-Hg**. Produced using the ESMValTool, version 2.0a1, recipe_drought_events.yml.

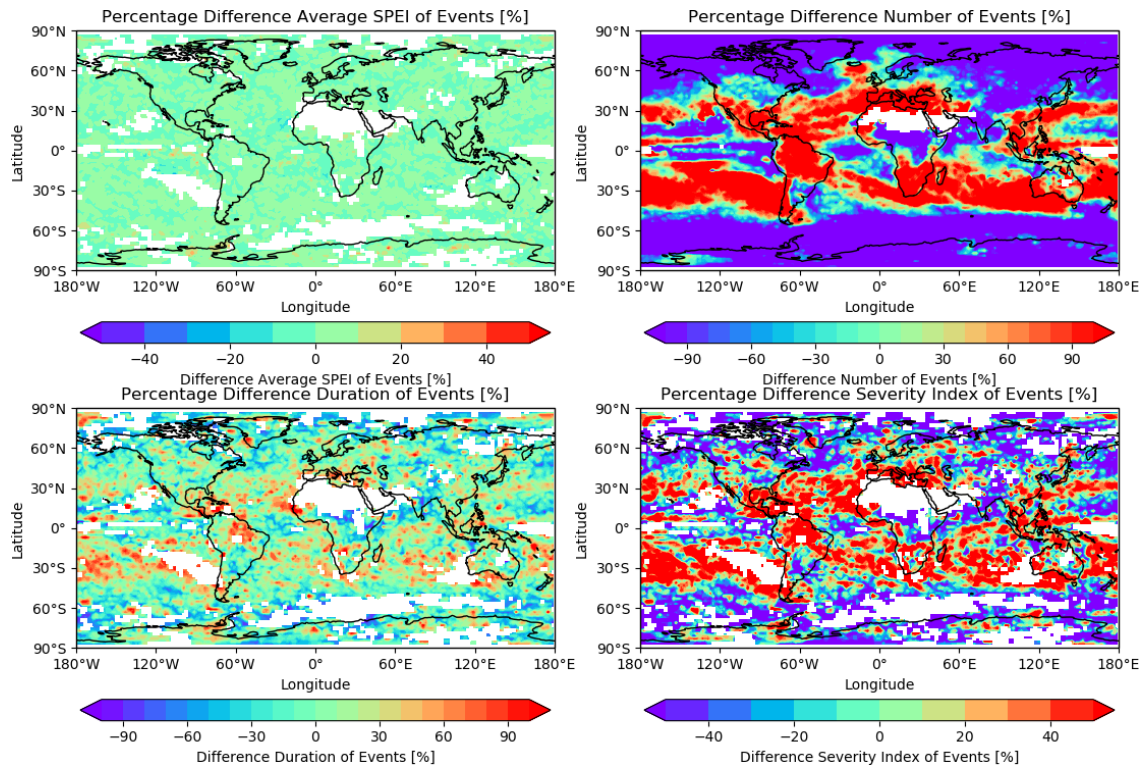


Figure 6-3: Same as Figure 6-1 but calculated based on **SPEI-PM**. Produced using the ESMValTool, version 2.0a1, recipe_drought_events.yml.

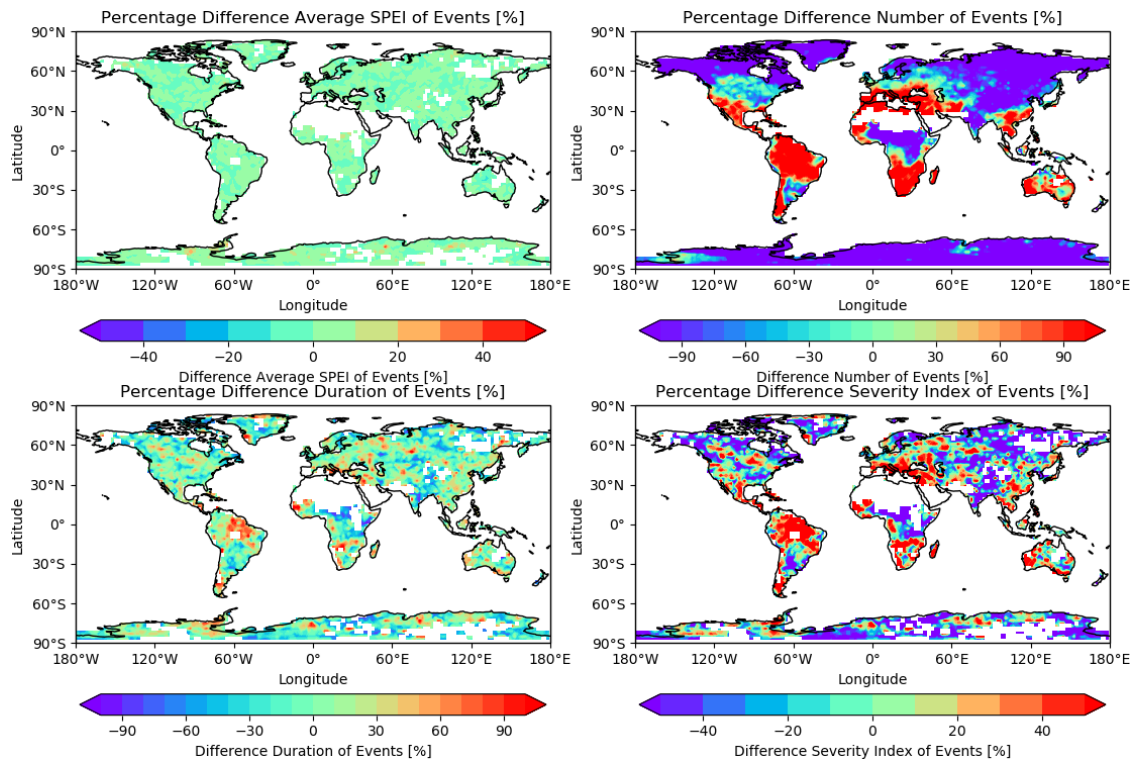


Figure 6-4: Same as Figure 6-1 but calculated based on **the internal PET variable from the individual models**. Produced using the ESMValTool, version 2.0a1, recipe_drought_events.yml.

The percentage difference for the number of drought events between model simulations for SSP5-85 (2050-2100) and historical (1950 to 2000) simulations is much higher when PET is calculated based on SPEI-Th (Fig 6-1) and slightly higher when calculated based on SPEI-Hg (Fig 6-2) in comparison with calculation based on SPEI-PM (Fig 6-3). Results from the internal PET variable (Fig 6-4) from the models covers land only while results from SPEI-Th, SPEI-Hg, and SPEI-PM cover both land and oceans.

SPEI-Th (Fig. 6-1) has no data for the change of average SPEI, duration and severity over large parts of the tropical and subtropical area, because there are no drought events detected between 1950 and 2000. SPEI-Hg (Fig 6-2) projects an increase of more than 100% in drought frequency throughout the continents except in above 60°N. The duration of events is projected to increase on average by about 50% and the severity index by over 50% while the average SPEI remains the same. SPEI-PM and direct PET (Fig 6-3 and 6-4) project almost a 100% increase in frequency of events in some part of the United States, South America, Southern Africa, Southern Europe and Australia. Duration and severity of events is projected to increase in the future on average by about 30% and the average SPEI remains the same.

Comparing the land distribution of the percentage differences, results from SPEI-Th project a contrasting result from the other methods, and SPEI-Hg overestimates the increase in the future scenario because besides precipitation, it is calculated based on minimum and maximum temperature only [G Hargreaves and Allen, 2003]. Results from SPEI-PM and the internal model variable for PET on the other hand agree very well.

SPEI-PM can be calculated using various approximations. For this work, SPEI-PM was initially calculated using the surface down-welling incident short wave radiation (*i.e.* *rsds*) alongside other variables (see Section 4.2.2). It was finally calculated using the cloud cover (*clt*) approximation. The results using *rsds* were very similar to those using *clt* (not shown), hence *clt* was used as it is available for more observational data sets compared to *rsds*. Also, relative humidity was included in the calculation of SPEI-PM, and almost the same result was produced. To use fewer variables, SPEI-PM calculation in this work was done without relative humidity. In this case, the SPEI-R package estimates the saturation water pressure from the minimum temperature instead of the relative humidity.

Based on the comparison with the internal model variable for PET, it is concluded that for the estimation of PET, the PM equation and thus the SPEI-PM is the best approximation. Therefore, in the subsequent analysis of drought characteristics for all available CMIP6 models only the SPEI-PM will be used. This confirms earlier studies where the SPEI-PM is considered the best approach for characterizing drought events for future simulation as well [Allen *et al.*, 1998]. This can be attributed to it being based on several other variables which contributes to the earth system in addition to precipitation, such as cloud cover, pressure, radiation, surface wind speed, as well as minimum and maximum temperature and pressure.

6.2. HISTORICAL CHANGES IN DROUGHT INDICES

The upper panels of figures 6-5 and 6-6 shows the probability for the different precipitation deficit and excess categories (see Table 4-1) for global data from 1979 to 2014 for SPI and SPEI-PM respectively. Each of the 7CMIP6 models is shown individually, alongside data from the ERA-Interim. The lower panels show the difference between the historical simulations and ERA-Interim.

This work focuses on drought events, which are extremely dry deficits. Looking at SPI (Fig. 6-5), most models (5) show a smaller probability for extremely dry and wet events and a higher probability for no-extreme events than ERA-Interim. For neutral events the results for the models compared to the ERA-Interim are not uniform for both SPI and SPEI-PM. SPI shows more extremely dry and wet events than SPEI-PM. This may be attributed to SPI's sole dependence on precipitation. Overall, ERA-Interim and models are in good agreement based on the absolute difference (lower figure) between them.

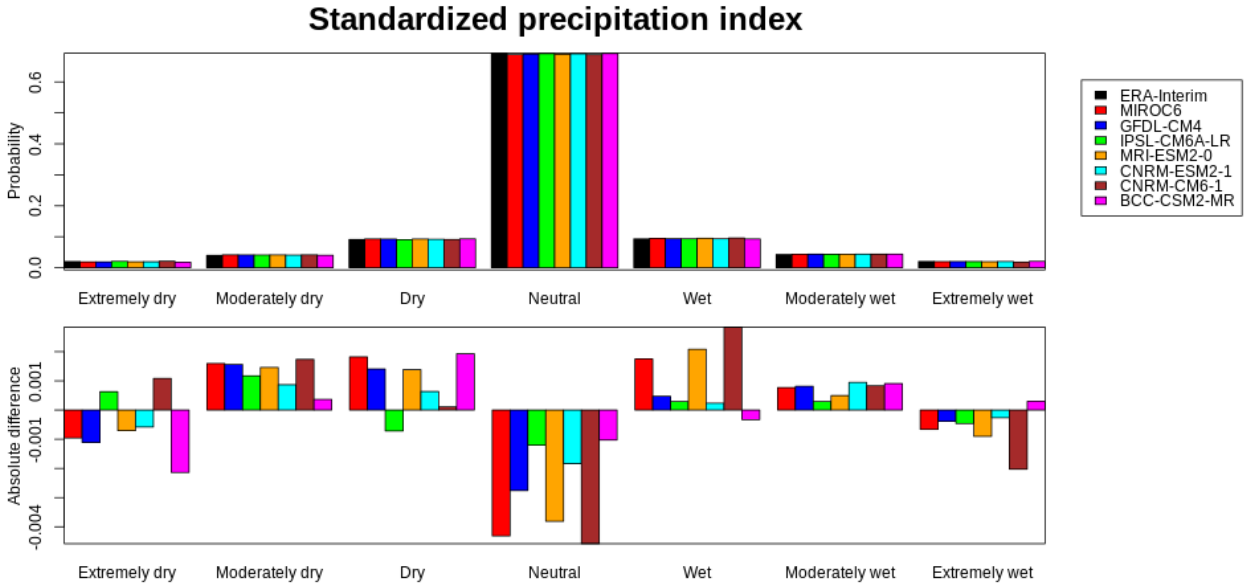


Figure 6-5: Histogram plot of SPI from the ERA-Interim observation (black) and the historical simulations from 7 CMIP6 models (colours) between 1979 and 2014 [upper panel] and their difference [lower panel]. (Produced using the ESMValTool, version 2.0a1, recipe_spikeah_histogram.yml)

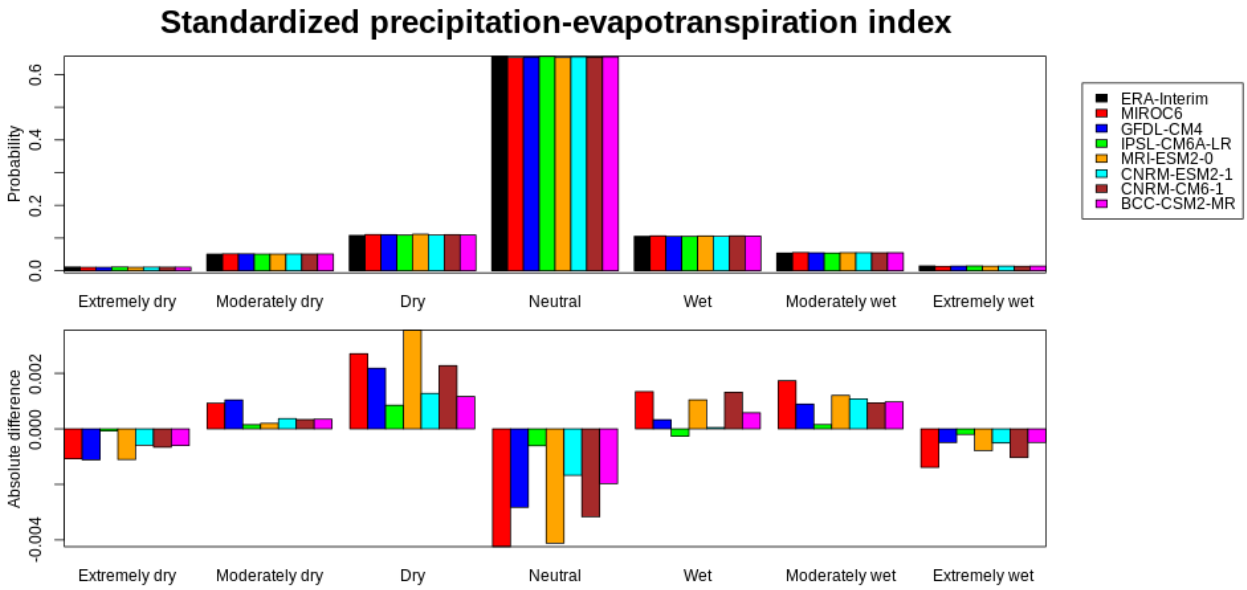


Figure 6-6: Histogram plot of SPEI-PM from the ERA-Interim observation (black) and the historical simulations from 7 different CMIP6 models (colours) between 1979 and 2014 [upper panel] and their difference [lower panel]. (Produced using the ESMValTool, version 2.0a1, recipe_spei_histogram_area.yml)

The main characteristics of drought events from SPI and SPEI-PM based on ERA-Interim and the historical multi-model mean for the time period 1979 - 2014 is shown in Appendix Figures A1 and A2, respectively. The average SPI for ERA-Interim (see Figure A1, left), spans from -2.0 to -2.8. The average SPI in Europe, Russia, Australia, Canada and Southern Africa is -2.4 with a higher index of -2.6 over the oceans. The number of drought events per year (frequency) is highest in these regions with a record of 0.15 to 0.25 and as low as 0.10 in Central Africa. The duration of events in these regions including Asia is relatively estimated to be about 2 to 3 months while the highest duration of 6 months is observed in the areas with the lower frequency of events such as Southern America (Brazil, Venezuela and Columbia), Central Africa and some part of Greenland. This corresponds with the study done by *Penalba and Rivera* [2013] over Southern South America. Where it was recorded that areas where the occurrence of droughts is more (less) common correlates with regions with a shorter (longer) duration. The severity index in these regions are also on the high side of about 7 to 8.

In the ERA-Interim using SPEI-PM (Figure A1, right), the average SPEI is majorly -2.2 over the lands and oceans. Number of events per year (frequency) is estimated between 0.05 to 0.20. The number of events in Central Africa, Brazil, United states of America is low compared to the rest of the world. A higher number of 0.20 is observed in Canada, Greenland, Asia and Russia. The duration of events in Canada and Russia is less than 3 months while duration of events in other region is between 3 and 6 months. The severity index follows the same pattern with results using SPI, that is regions with higher duration have a higher severity of between 6 and 7 while regions of lower duration have a lesser severity of between 2 and 3 of events. The duration of events over the oceans is relatively high with a record of more than 6 months. Drought events in the united states of America, South Southern America, Europe and Asia lasted between 4 and 6 months.

The main characteristics of drought events from SPI and SPEI-PM based on 7 CMIP6 models is shown also in Figure A2, with some differences. To account for the difference between the ERA-Interim and the 7 CMIP6 models quantitatively, a percentage difference of these characteristics are shown in Figure 6-7 using SPI (left) and SPEI-PM (right). For this comparison, the precipitation and other variables from the model data is interpolated to the same grid as the ERA-Interim before calculating the SPI and SPEI. The multi-model mean is calculated for drought

characteristics (frequency, duration, average SPI and severity index). Generally, the percentage difference between ERA-Interim observations and the SPI multi-model mean is very small, except for specific regions. The percentage difference (between the observation and the models) average SPI for drought events is even, except for a part of Brazil, central Africa, Pacific Ocean and the Indian ocean with about 30% overestimation from the multi-model mean. The frequency of events is also similar in most regions except in Central Africa, Columbia and the Pacific Ocean. The duration of events is relatively similar in North America and Russia with about 0% to 30% except a spike of 60 to 90% in the West Africa, USA and Brazil. The multi-model mean over estimates the duration and severity of events over the ocean by almost 60% and 50% respectively. For SPEI-PM, the percentage difference of average SPEI is the same across the world, the number of events is similar in most regions with percentage difference between -20% and 60%, however the multi-model mean shows a lower number of events in Central Africa, Columbia, and some parts of USA by almost -90%. The percentage difference of duration and severity of events is very similar to the results produced using SPI. Generally, a good similarity is found in the percentage difference of the main drought characteristics performed between the observations and multi-model mean using SPI and SPEI-PM.

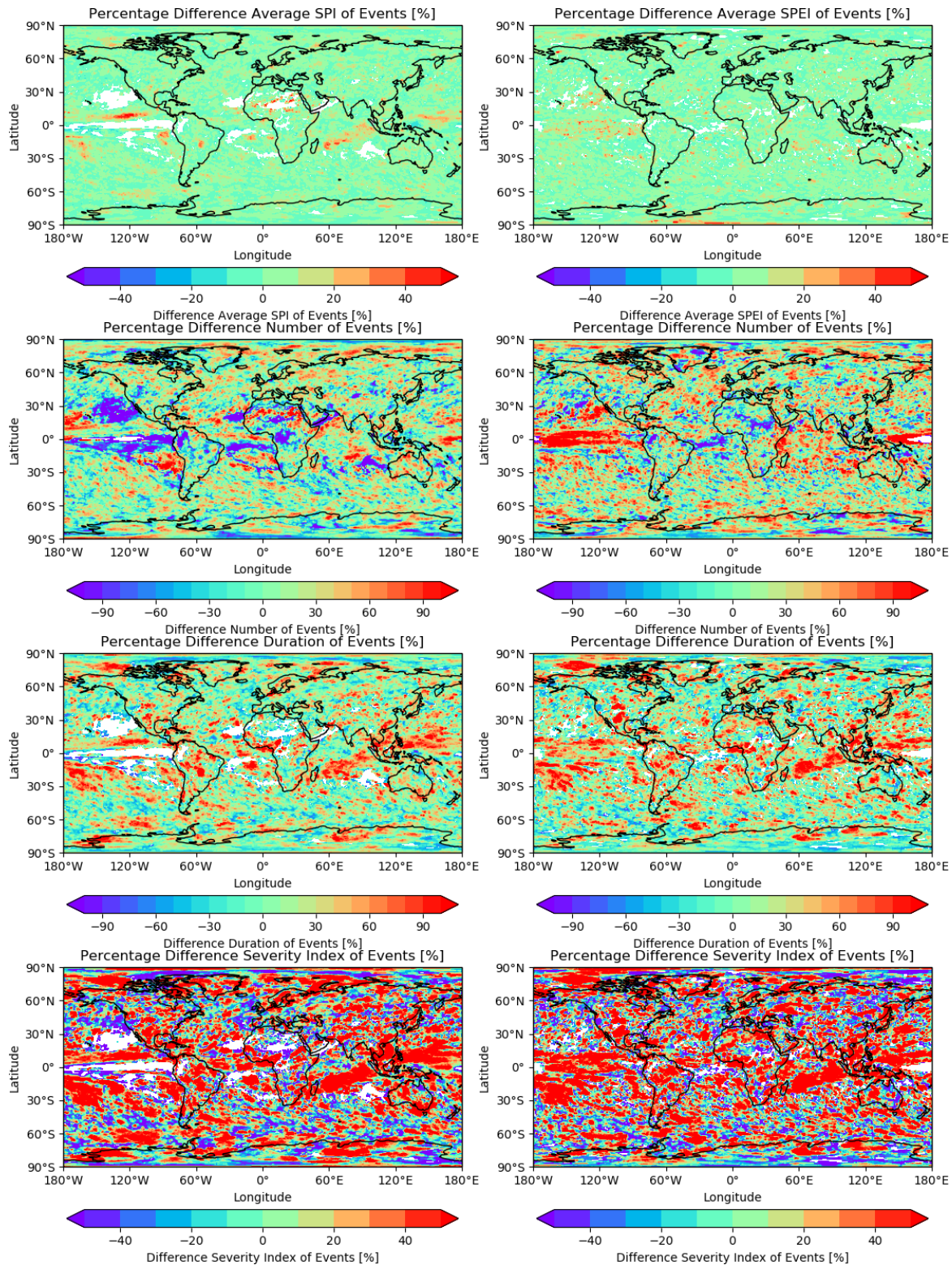


Figure 6-7: Percentage difference between multi-model mean of ERA-Interim observations (1979 to 2014) and 7 CMIP6 models historic simulations (1979 to 2014) showing average SPI/SPEI, number, duration and severity index of drought events using the SPI (left) and SPEI-PM (right). Produced using the ESMValTool, version 2.0a1, recipe_drought_events.yml.

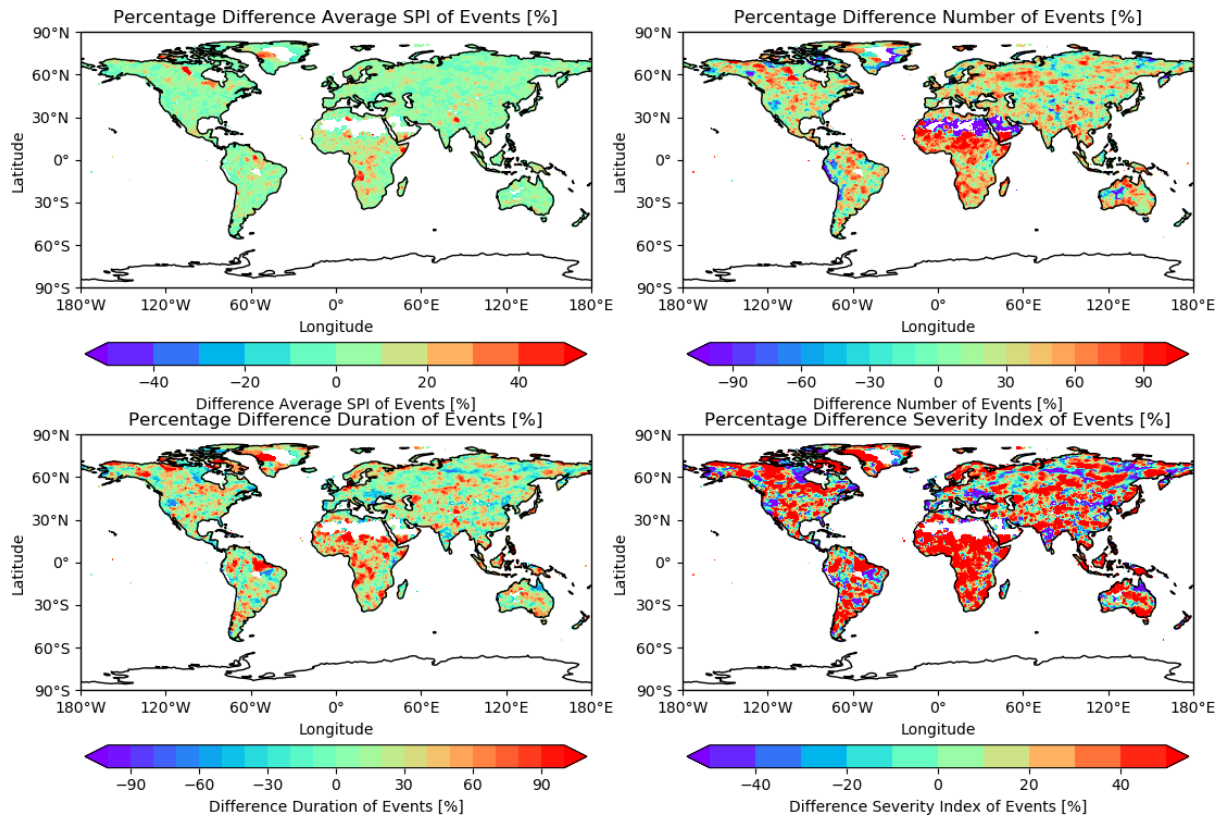


Figure 6-7: Percentage difference between multi-model mean of CRU observations (1979 to 2014) and 7 CMIP6 models historic simulations (1979 to 2014) showing average SPI/SPEI, number, duration and severity index of drought events using the SPI. Produced using the ESMValTool, version 2.0a1, recipe_drought_events.yml.

Results from the produced map plots (Figures A1 and A2) show that the 7 CMIP6 multi-model mean is slightly different from the ERA-Interim observations. This confirms the absolute difference (lower figure from the histogram plots, Fig 6-5 and 6-6) where the CMIP6 models simulate varying difference with the ERA-Interim. Overall, good agreement is found for the differences between models and observations for SPI and SPEI-PM. This is shown from the percentage difference (Fig. 6-7) calculated between the observations and CMIP6 models.

A percentage difference (Fig. 6-8) between the multi-model mean of the historical model simulations and CRU observations was also calculated, following the same approach as with the ERA-Interim. For this comparison, the precipitation variable from the model data was interpolated to the same grid as the CRU data. Results produced for average SPI, duration and severity index are very similar to the percentage difference calculated for the ERA-Interim data. The major difference however shows that the CRU finds a higher number of drought events than the CMIP6 models especially in central Africa and lesser events in the Northern Africa.

6.3. HISTORICAL AND FUTURE CHANGES IN DROUGHT CHARACTERISTICS

In this section, projected changes in drought characteristics are studied for the future simulations (2050-2100) using the SSP5-85 scenario by comparing it with the historical multi-model mean (1950-2000) using SPI and SPEI-PM. For both histograms and map plots SPI and SPEI-PM are calculated for the complete time series 1950-2100 first, see section 6.1.

Results from the histogram plots (Fig. 6-9 and 6-10) show the global simulations of drought events using SPI and SPEI-PM. Comparing historic histogram plot with future scenario SSP5-85, fewer events are projected for $SPI < 0$ and more events with $SPI > 0$ especially the number of pluvial events ($SPI > 2$). For SPEI-PM, there are more drought events with $SPEI > 1$. The number of drought events with SPEI between 0 and 1 decreases, while the number of events with $SPEI < -1$ stays almost the same. This result suggests that the number of drought events decreases globally.

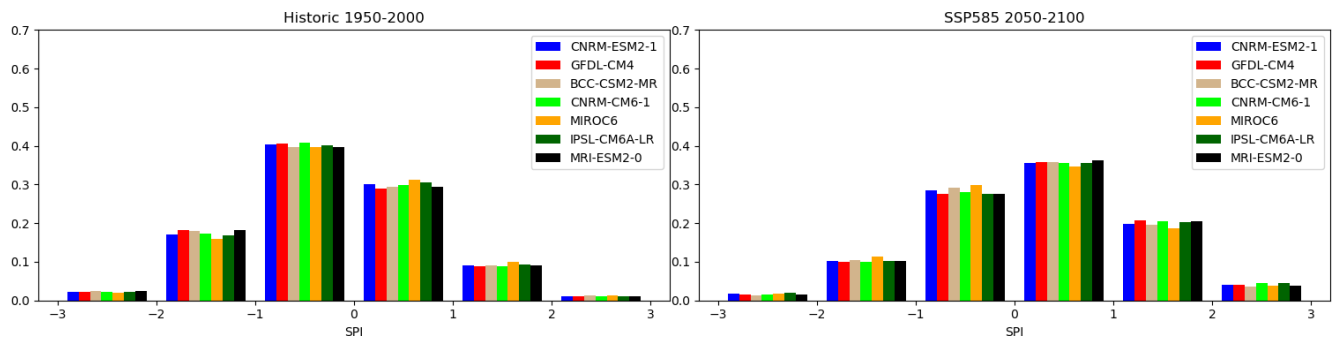


Figure 6-9 Histogram plot showing the historical (1950 - 2000) and future (2050 - 2100) simulations from 7 CMIP6 models using SPI. Produced using the ESMValTool, version 2.0a1, recipe_spikeah_histogram.yml

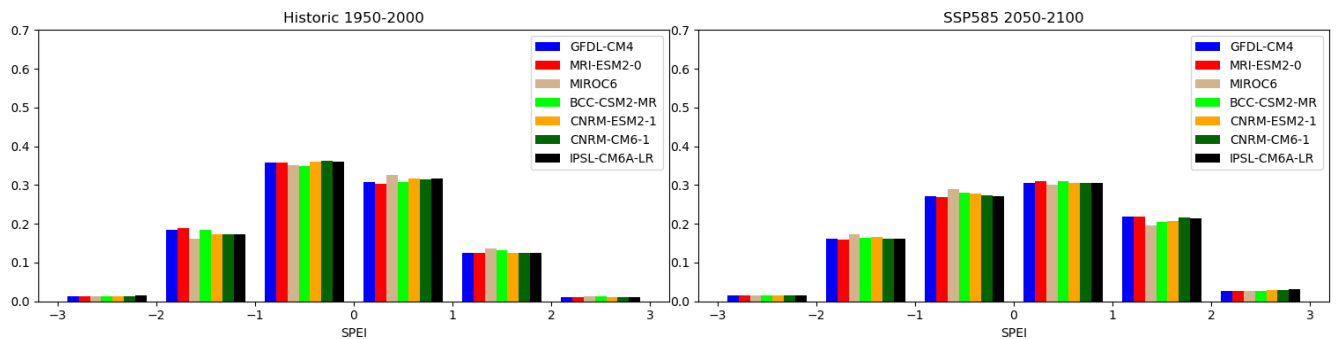


Figure 6-8: Histogram showing the historical (1950 - 2000) and future (2050 - 2100) simulations from 7 CMIP6 models using SPEI-PM. Produced using the ESMValTool, version 2.0a1, recipe_spei_PM_histogram_area.yml.

The multi-model mean of the historical simulations calculated from 7 CMIP6 models is shown in Figure A3. The results are very different from the ones shown in Figure A2. For FigureA3, the

SPI and SPEI-PM were calculated for the time period between 1950 – 2100 and the figure shows the result for the partial time series between 1950 and 2000. For Figure A2, SPI and SPEI-PM were calculated for the complete time series between 1979-2014. The difference between these figures mainly comes from the use of the partial time series which underlines the importance of calculating SPI and SPEI-PM for 1950-2100 to compare historical and future simulations (see also Figure 6.1). Additionally, the different time period 1979-2014 versus 1950-2000 and grid can cause differences. The precipitation and other variables from the model data is regridded to a common 2 degrees' horizontal resolution before calculating the SPI and SPEI-PM. For the drought events in historical simulations, (Figure A3, left) an average SPI of -2.4 is recorded across the continents. The number of drought events between (0.15 to 0.25 per year) is found in Canada, Russia, some part of Europe, USA and Brazil with an average duration of 3 months, and a severity index of 3 to 5. A lower number of events (0.05 per year) is recorded in Northern Africa, and over the oceans (Pacific, Atlantic and Indian), with an average duration of 2 months, an average SPI of -2.4, and a severity index of 2 are simulated. For the historical simulations using SPEI-PM, (Figure A3, right), the average SPEI is majorly -2.2 with a spike of -2.4 in Northern Canada, a part of Russia and the Pacific Ocean. No drought event was found in the Northern Africa. Number of drought events found close to the equator (USA, South America, South Africa, Australia, Europe, Asia) is relatively low with a record of between 0.05 to 0.15. A higher frequency of events is observed close to the poles (Northern Canada, Russia and Greenland). The duration of both events is between 1 and 3 months with a spike of about 4 to 5 months in a part of Brazil, Southern Africa and Pacific Ocean. The severity index is generally between 2 and 3.

For the SSP5-85 (scenario) multi-model mean, the time period between 2050 – 2100 is selected from the complete time series of 1950-2100. Figure A4 (left) projects a high number of drought events and durations for the United States of America, South America (Brazil, Guyana, Venezuela, Chile), Southern Europe, parts of Asia, Southern Africa and Southern Australia. These events are projected with a duration of 3 months, an average SPI of -2.6 in the specific regions, and a severity index of between 2 and 5. The future scenario (Figure A4, right) simulates a more intense result to the observation with an average SPI of -2.2 and a higher index of -2.4 in Northern Canada, Greenland, Russia, Central Africa and -2.6 in Atlantic Ocean. The number of events around the equator reflect a contrasting result with the observation. That is,

more drought events per year (frequency) are observed around the equator, about 0.25 to 0.30 and a lesser frequency of events of about 0.10 and 0.15 is observed around the Southern and Arctic Ocean. The duration of events lasted about 3 months except in the North Western Africa (Algeria, Niger, Mali), a part of USA and South America (Venezuela, Brazil and Columbia) which records a duration of 4 months. The severity index spans between 4 and 6 with the same pattern as the regions where duration of events is high.

A percentage difference between future and historical simulations was calculated for the 7 CMIP6 models and results are shown in Figure 6-11 for SPI (left) and SPEI-PM (right). The average SPI is largely the same, except in Central Africa, where average SPI increased slightly by 20%. The number of events will increase by almost 200% in certain regions (parts of Europe, United states, Southern America and Southern Africa) around the equator in the future while regions close to the pole will observe lesser or no drought events. The duration of events increased slightly by 40% and the severity index increases also by 40%. The average SPEI remains the same, the number of events per year (frequency) will increase by almost 200% occupying entire equator and lesser frequency of drought events close to the poles.

Based on the differences between the SSP5-85 and the historical multi-model mean, it can be concluded that there is a higher number of drought events in the subtropical and mid-latitude regions in the future, although with same average SPI and SPEI but increased duration and severity index in specific locations. The frequency of events from the SPEI-PM shows a higher increase compared to SPI. Even though SPI found more events in the historical simulations, it found few more events in the future. SPEI-PM on the other hand found fewer events in its historical simulations and projects higher frequency of events in its future simulations hence the 200% increase. Results from the multi-model mean also show that regions with already dry conditions are much more likely to show a higher number of drought events for the SSP5-85 scenario. This confirms the dry gets dryer and the wet gets wetter (DDWW) paradigm [Greve *et al.*, 2014].

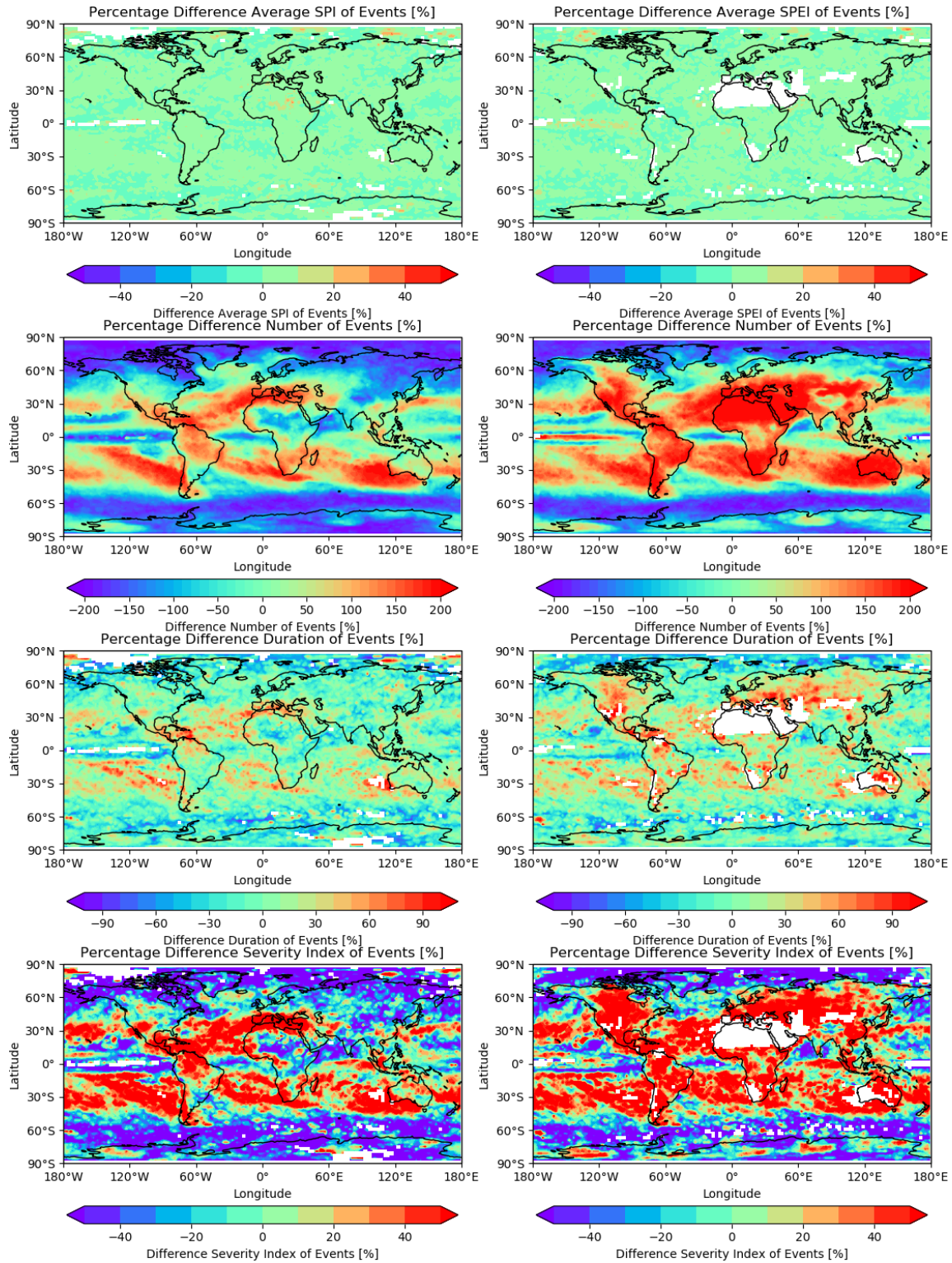


Figure 6-91: Percentage difference of 7 CMIP6 models showing average SPI/SPEI, frequency, duration and severity of drought events using SPI (left) and SPEI-PM (right) between the historic (1950 to 2100) and SSP5-85 (2050-2100) multi-model mean. Produced using the ESMValTool, version 2.0a1, recipe_drought_events.yml.

7. SUMMARY AND OUTLOOK

In this thesis an analysis of drought events characterized by average number, frequency, duration and severity in historical and future simulations performed with the new generation of Earth system models (ESMs) participating in the Coupled Model Intercomparison Project (CMIP6) is presented. The results are drawn on calculations with different drought indices, in particular the Standardized Precipitation Index (SPI) and the Standardized Precipitation Evapotranspiration Index (SPEI). While SPI is calculated using precipitation only, SPEI additionally includes potential evapotranspiration (PET) which is approximated using methods of different complexity: SPEI-Th based on temperature only, SPEI-Hg based on monthly mean daily minimum and maximum temperature and SPEI-PM additionally taking into account cloud cover, air pressure and wind speed.

Although limitations for the SPEI calculations based on temperature-based methods are known, they are often used due to a lack of available variables. Additionally, the evidence for this limitations is not strong enough in verification of different SPEI methods that are restricted to the historical period. However, as this thesis shows these limitations become significant under climate change projections under the SSP5-8.5 forcing scenario.

Here, three CMIP6 models with all necessary variables for the calculations of SPEI-Th, SPEI-Hg and SPEI-PM that additionally provided PET as simulated model variable were used to compute SPEI and to compare the different methods. A comparison of changes in drought characteristics from historical to SSP5-85 scenarios for these models show that only SPEI-PM reproduces the results based on the model's PET variable well. SPEI-Th overestimates the increase in the frequency of drought events severely, showing a large near-global increase. SPEI-Hg projects a stronger increase in drought frequency compared to SPEI using the internal model variable PET for the subtropics and mid-latitudes. For SPEI-PM the drought frequency increases moderately for subtropical regions, which is similar to the results produced using the internal PET variable. It can therefore be concluded that the SPEI-PM is the best approach when using SPEI and is used for all following analysis of SPEI in this thesis.

A further evaluation and comparison of SPI and SPEI-PM was performed using the ERA-Interim and the CRU datasets with the historical runs from 7 CMIP6 models for the time period 1979 to 2014. The resulting histograms of SPI and SPEI-PM show small differences between these data

sets and the CMIP6 models. SPI shows a slightly higher frequency of extreme events than SPEI-PM in the historical runs. For both indices the probability for extreme drought and pluvial event as well as neutral events is higher for ERA-Interim data than for most of the model simulations, while the models have a slightly higher probability for moderate dry and wet events. For SPEI-PM and SPI, the percentage difference for the drought characteristics between the multi-model mean of the historical CMIP6 simulations and ERA-Interim data is small for most regions and agrees well with each other. SPI using the CRU dataset yields a similar result, except for the frequency of events.

Furthermore, changes in drought characteristics were calculated for 7 CMIP6 models using SPI and SPEI-PM comparing averages for 1950-2000 and 2050-2100 of a combined time series from 1950 to 2100, using historical and future simulations with the SSP5-85 scenario. SPI shows a higher frequency of drought events in both the historical and future simulations than SPEI-PM, which in turn has a larger increase of drought events from the historical to the future simulations. In the already dry subtropics, the increase is over 150% and 30% using SPI for frequency and severity, respectively. For SPEI-PM the same characteristics increase by 200% and 50% in this region.

The calculation of the SPI and SPEI-TH was done with existing routines that were already implemented in the Earth System Model Evaluation Tool (ESMValTool) version 1.0. Other SPEI methods (i.e. the SPEI-PM and SPEI-Hg) were initially not available in the ESMValTool, but have been included in the ESMValTool as part of this thesis. The results for the changes in the drought characteristics based on SPI from this thesis were contributed to one of the four ESMValTool version 2.0 papers (Weigel et al. (including Adeniyi), 2019).

While this thesis focused on drought events, a similar analysis could be applied to changes in the future pluvial characteristics (frequency, duration, and severity index) based on CMIP6 simulations using SPI and SPEI-PM. Additionally, more CMIP6 models could be included in the analysis as they become available to provide more robust conclusions on changes of drought events as these data sets become available. In addition, the study could be extended by analyzing climate projections from ScenarioMIP under different forcing scenarios [O'Neill et al., 2016]. Furthermore, machine learning techniques could provide a powerful tool to supplement the classic indices like SPI and SPEI for the detection of droughts and other extreme events.

REFERENCES

- AghaKouchak, A., L. Y. Cheng, O. Mazdiyasni, and A. Farahmand (2014), Global warming and changes in risk of concurrent climate extremes: Insights from the 2014 California drought, *Geophys Res Lett*, *41*(24), 8847-8852, doi:10.1002/2014gl062308.
- Allen, R., L. Pereira, and M. Smith (1998), *Crop evapotranspiration-Guidelines for computing crop water requirements-FAO Irrigation and drainage paper 56*.
- Barriopedro, D., C. M. Gouveia, R. M. Trigo, and L. Wang (2012), The 2009/10 Drought in China: Possible Causes and Impacts on Vegetation, *J Hydrometeorol*, *13*(4), 1251-1267, doi:10.1175/JHM-D-11-074.1.
- Beguieria, S., S. M. Vicente-Serrano, F. Reig, and B. Latorre (2014), Standardized precipitation evapotranspiration index (SPEI) revisited: parameter fitting, evapotranspiration models, tools, datasets and drought monitoring, *Int J Climatol*, *34*(10), 3001-3023, doi:10.1002/joc.3887.
- Burke, E. J., and S. J. Brown (2008), Evaluating Uncertainties in the Projection of Future Drought, *J Hydrometeorol*, *9*(2), 292-299, doi:10.1175/2007JHM929.1.
- Chen, D., G. Gao, C.-Y. Xu, J. Guo, and G. Ren (2005), Comparison of the Thornthwaite method and pan data with the standard Penman-Monteith estimates of reference ET in China, *CLIMATE RESEARCH*, *28*, 123-132, doi:10.3354/cr028123.
- Cheng, L., M. Hoerling, A. AghaKouchak, B. Livneh, X.-W. Quan, and J. Eischeid (2016), How Has Human-Induced Climate Change Affected California Drought Risk?, *Journal of Climate*, *29*(1), 111-120, doi:10.1175/jcli-d-15-0260.1.
- Dai, A. (2012), Increasing drought under global warming in observations and models, *Nature Climate Change*, *3*, 52, doi:10.1038/nclimate1633
- Dee, D. P., et al. (2011), The ERA-Interim reanalysis: configuration and performance of the data assimilation system, *Q J Roy Meteor Soc*, *137*(656), 553-597, doi:Doi 10.1002/Qj.828.
- Droogers, P., and R. G. Allen (2002), Estimating Reference Evapotranspiration Under Inaccurate Data Conditions, *Irrigation and Drainage Systems*, *16*(1), 33-45, doi:10.1023/A:1015508322413.
- Dubrovský, M., M. Svoboda, M. Trnka, M. Hayes, D. Wilhite, Z. Zalud, and P. Hlavinka (2009), Application of relative drought indices to assess climate change impact on drought conditions in Czechia, *Theoretical and Applied Climatology*, *96*, 155-171, doi:10.1007/s00704-008-0020-x.
- E. Taylor, K., S. Ronald, and G. Meehl (2011), An overview of CMIP5 and the Experiment Design, *Bulletin of the American Meteorological Society*, *93*, 485-498, doi:10.1175/BAMS-D-11-00094.1.
- Eyring, V., S. Bony, G. A. Meehl, C. A. Senior, B. Stevens, R. J. Stouffer, and K. E. Taylor (2016a), Overview of the Coupled Model Intercomparison Project Phase 6 (CMIP6) experimental design and organization, *Geosci. Model Dev.*, *9*(5), 1937-1958, doi:10.5194/gmd-9-1937-2016.

Eyring, V., et al. (2016b), ESMValTool (v1.0) – a community diagnostic and performance metrics tool for routine evaluation of Earth system models in CMIP, *Geosci. Model Dev.*, 9(5), 1747-1802, doi:10.5194/gmd-9-1747-2016.

Fita, L., J. Polcher, T. M. Giannaros, T. Lorenz, J. Milovac, G. Sofiadis, E. Katragkou, and S. Bastin (2019), CORDEX-WRF v1.3: development of a module for the Weather Research and Forecasting (WRF) model to support the CORDEX community, *Geosci. Model Dev.*, 12(3), 1029-1066, doi:10.5194/gmd-12-1029-2019.

Fuchs, M. S. a. B. A. (2016), World Meteorological Organization (WMO) and Global Water Partnership (GWP), , *Handbook of Drought Indicators and Indices, Integrated Drought Management Programme (IDMP), Integrated Drought Management Tools and Guidelines Series 2. Geneva.*

Greve, P., B. Orlowsky, B. Mueller, J. Sheffield, M. Reichstein, and S. Seneviratne (2014), Global assessment of trends in wetting and drying over land, *Nature Geoscience*, 7, doi:10.1038/ngeo2247.

Guenang, G., and M. Francois (2014), Computation of the Standardized Precipitation Index (SPI) and Its Use to Assess Drought Occurrences in Cameroon over Recent Decades, *Journal of Applied Meteorology and Climatology*, 53, 2310-2324, doi:10.1175/JAMC-D-14-0032.1.

Gutowski Jr, W. J., et al. (2016), WCRP COordinated Regional Downscaling EXperiment (CORDEX): a diagnostic MIP for CMIP6, *Geosci. Model Dev.*, 9(11), 4087-4095, doi:10.5194/gmd-9-4087-2016.

Guttman, N. B. (1994), On the Sensitivity of Sample L Moments to Sample Size, *Journal of Climate*, 7(6), 1026-1029, doi:10.1175/1520-0442(1994)007<1026:Otsosl>2.0.Co;2.

Hagman, G., H. Beer, and k. Svenska röda (1984), *Prevention better than cure : report on human and environmental disasters in the Third World*, Swedish Red Cross, Stockholm.

Hargreaves George, H., and R. G. Allen (2003), History and Evaluation of Hargreaves Evapotranspiration Equation, *Journal of Irrigation and Drainage Engineering-asce - J IRRIG DRAIN ENG-ASCE*, 129, doi:10.1061/(ASCE)0733-9437(2003)129:1(53).

Hargreaves George, H., and Z. A. Samani (1982), Estimating Potential Evapotranspiration., *Journal of Irrigation and Drainage Division*,, 108 (103), 225–230.

Hargreaves, G. L. (1983), Water requirements and agricultural benefits for the Senegal river basin,"Thesis submitted in partial fulfillment of the degree of Master of Science in Engineering," Utah State Univ., Logan, Utah, 111.

Harris, I., P. Jones, T. Osborn, and D. Lister (2014), Updated high-resolution grids of monthly climatic observations—The CRU TS3.10 Dataset, *Int J Climatol*, 34, n/a-n/a, doi:10.1002/joc.3711.

Hayes, M., M. Svoboda, N. Wall, and M. Widhalm (2011), The Lincoln Declaration on Drought Indices: Universal Meteorological Drought Index Recommended, *Bulletin of the American Meteorological Society*, 92(4), 485-488, doi:10.1175/2010bams3103.1.

Hilario, F., R. de Guzman, D. Ortega, P. Hayman, and B. Alexander (2009), El Niño Southern Oscillation in the Philippines: Impacts, Forecasts, and Risk Management, *Philipp. J. Dev.*, 36, 9-34.

Hubbart, J., and M. Pidwirny (2010), *Hydrologic Cycle*, edited.

IPCC (2012), *Managing the Risks of Extreme Events and Disasters to Advance Climate Change Adaptation. A Special Report of Working Groups I and II of the Intergovernmental Panel on Climate Change* [Field, C.B., V. Barros, T.F. Stocker, D. Qin, D.J. Dokken, K.L. Ebi, M.D. Mastrandrea, K.J. Mach, G.-K. Plattner, S.K. Allen, M. Tignor, and P.M. Midgley (eds.)]. , *Cambridge University Press, Cambridge, UK and New York, NY, USA*,, 582 pp.

IPCC (2014a), *Climate Change 2014: Impacts, Adaptation, and Vulnerability. Part A: Global and Sectoral Aspects. Contribution of Working Group II to the Fifth Assessment Report of the Intergovernmental Panel on Climate Change* [Field, C.B., V.R. Barros, D.J. Dokken, K.J. Mach, M.D. Mastrandrea, T.E. Bilir, M. Chatterjee, K.L. Ebi, Y.O. Estrada, R.C. Genova, B. Girma, E.S. Kissel, A.N. Levy, S. MacCracken, P.R. Mastrandrea, and L.L. White (eds.)]. *Cambridge University Press, Cambridge, United Kingdom and New York, NY, USA*,, 1132 pp.

IPCC (2014b), *Climate Change 2014: Synthesis Report. Contribution of Working Groups I, II and III to the Fifth Assessment Report of the Intergovernmental Panel on Climate Change* [Core Writing Team, R.K. Pachauri and L.A. Meyer (eds.)]. , IPCC, Geneva, Switzerland, 151 pp.

IPCC (2018), *Summary for Policymakers. In: Global Warming of 1.5°C. An IPCC Special Report on the impacts of global warming of 1.5°C above pre-industrial levels and related global greenhouse gas emission pathways, in the context of strengthening the global response to the threat of climate change, sustainable development, and efforts to eradicate poverty* [Masson-Delmotte, V., P. Zhai, H.-O. Pörtner, D. Roberts, J. Skea, P.R. Shukla, A. Pirani, W. Moufouma-Okia, C. Péan, R. Pidcock, S. Connors, J.B.R. Matthews, Y. Chen, X. Zhou, M.I. Gomis, E. Lonnoy, T. Maycock, M. Tignor, and T. Waterfield (eds.)]. , *World Meteorological Organization, Geneva, Switzerland*,, 32 pp.

Kan, M., A. Kan, and C. Oğuz (2017), *Ecosystem-Based Approach to Combat Drought and Desertification and Their Relation with Rural Development*, edited, pp. 319-342.

Kiem, A., et al. (2016), *Natural hazards in Australia: droughts*, *Climatic Change*, doi:10.1007/s10584-016-1798-7.

Lewis, S. L., P. M. Brando, O. L. Phillips, G. M. F. van der Heijden, and D. Nepstad (2011), *The 2010 Amazon Drought*, *Science*, 331(6017), 554, doi:10.1126/science.1200807.

Li, Y., y. wei, w. meng, and X. Yan (2009), *Climate change and drought: A risk assessment of crop-yield impacts*, *Climate Research*, 39, 31-46.

Lloyd-Hughes, B., and M. A. Saunders (2002), *A Drought Climatology for Europe*, *Int J Climatol*, 22, 1571-1592, doi:10.1002/joc.846.

Lyon, B. (2014), *Seasonal Drought in the Greater Horn of Africa and Its Recent Increase during the March–May Long Rains*, *Journal of Climate*, 27(21), 7953-7975, doi:10.1175/JCLI-D-13-00459.1.

Lyon, B., H. Cristi, E. R. Verceles, F. D. Hilario, and R. Abastillas (2006), *Seasonal reversal of the ENSO rainfall signal in the Philippines*, *Geophys Res Lett*, 33(24), doi:10.1029/2006GL028182.

- Marengo, J. A., C. A. Nobre, J. Tomasella, M. D. Oyama, G. Sampaio de Oliveira, R. de Oliveira, H. Camargo, L. M. Alves, and I. F. Brown (2008), The Drought of Amazonia in 2005, *Journal of Climate*, 21(3), 495-516, doi:10.1175/2007JCLI1600.1.
- Martin, E. R. (2018), Future Projections of Global Pluvial and Drought Event Characteristics, *Geophys Res Lett*, 45(21), 11,913-911,920, doi:10.1029/2018GL079807.
- Masih, I., S. Maskey, F. E. F. Mussá, and P. Trambauer (2014), A review of droughts on the African continent: a geospatial and long-term perspective, *Hydrol. Earth Syst. Sci.*, 18(9), 3635-3649, doi:10.5194/hess-18-3635-2014.
- Mishra, A., and V. Singh (2010), A Review of Drought Concepts, *Journal of Hydrology*, 391, 202-216, doi:10.1016/j.jhydrol.2010.07.012.
- Mishra, A., V. Singh, and V. P (2009), Analysis of drought severity-area-frequency curves using a general circulation model and scenario uncertainty, *J. Geophys. Res.*, 114, doi:10.1029/2008JD010986.
- Mpelasoka, F., K. Hennessy, R. Jones, and B. Bates (2008), Comparison of suitable drought indices for climate change impacts assessment over Australia towards resource management, *Int J Climatol*, 28(10), 1283-1292, doi:10.1002/joc.1649.
- Nielsen-Gammon (2012), The 2011 Texas Drought (37).
- Nikam, B., P. Kumar, V. Garg, P. Thakur, and S. Aggarwal (2014), COMPARATIVE EVALUATION OF DIFFERENT POTENTIAL EVAPOTRANSPIRATION ESTIMATION APPROACHES, *International Journal of Research in Engineering and Technology*, 03, 544-552, doi:10.15623/ijret.2014.0306102.
- O'Neill, B. C., et al. (2016), The Scenario Model Intercomparison Project (ScenarioMIP) for CMIP6, *Geosci. Model Dev.*, 9(9), 3461-3482, doi:10.5194/gmd-9-3461-2016.
- Orlowsky, B., and S. I. Seneviratne (2012), Global changes in extreme events: regional and seasonal dimension, *Climatic Change*, 110(3), 669-696, doi:10.1007/s10584-011-0122-9.
- Penalba, O., and J. Rivera (2013), Future Changes in Drought Characteristics over Southern South America Projected by a CMIP5 Multi-Model Ensemble, *American Journal of Climate Change*, 2, 173-182, doi:10.4236/ajcc.2013.23017.
- Penman, H. L., and B. A. Keen (1948), Natural evaporation from open water, bare soil and grass, *Proceedings of the Royal Society of London. Series A. Mathematical and Physical Sciences*, 193(1032), 120-145, doi:10.1098/rspa.1948.0037.
- Peters, E. J. (2003), Propagation of drought through groundwater systems.
- Peters, E. J. (2014), Measuring the Severity of Dry Seasons in the Grenadines, , *The West Indian Journal of Engineering*,, 36(32), 42-50.
- Riahi, K., S. Rao, V. Krey, C. Cho, V. Chirkov, G. Fischer, G. Kindermann, N. Nakicenovic, and P. Rafaj (2011), RCP 8.5—A scenario of comparatively high greenhouse gas emissions, *Climatic Change*, 109(1), 33, doi:10.1007/s10584-011-0149-y.

- Sanjairaj, V., S. Iniyar, and R. Goic (2012), A Review of Climate Change, Mitigation and Adaptation, *Renewable and Sustainable Energy Reviews*, 16, 878–897, doi:10.1016/j.rser.2011.09.009.
- Shaw, S. B., and S. J. Riha (2011), Assessing temperature-based PET equations under a changing climate in temperate, deciduous forests, *Hydrological Processes*, 25(29), 1466-1478, doi:doi:10.1002/hyp.7913.
- Sheffield, J., and E. F. Wood (2008), Global Trends and Variability in Soil Moisture and Drought Characteristics, 1950–2000, from Observation-Driven Simulations of the Terrestrial Hydrologic Cycle, *Journal of Climate*, 21(3), 432-458, doi:10.1175/2007JCLI1822.1.
- Sheffield, J., E. F. Wood, and M. L. Roderick (2012), Little change in global drought over the past 60 years, *Nature*, 491, 435, doi:10.1038/nature11575. <https://www.nature.com/articles/nature11575>.
- Simmons, A., S. Uppala, Dee D, and S. Kobayashi (2006), ERA-Interim: New ECMWF reanalysis products from 1989 onwards., *ECMWF Newsletter*, 110: 126-135, doi:DOI 10.21957/pocnex23c6.
- Sippel, S., M. Reichstein, X. Ma, M. D. Mahecha, H. Lange, M. Flach, and D. Frank (2018), Drought, Heat, and the Carbon Cycle: a Review, *Current Climate Change Reports*, 4(3), 266-286, doi:10.1007/s40641-018-0103-4.
- Smakhtin, V. U., and E. L. F. Schipper (2008), Droughts: The impact of semantics and perceptions, *Water Policy*, 10(2), 131-143, doi:10.2166/wp.2008.036.
- Stagge, J. H., L. M. Tallaksen, C. Y. Xu, and H. A. J. Van Lanen (2014), Standardized precipitation-evapotranspiration index (SPEI): Sensitivity to potential evapotranspiration model and parameters,, *Int. J. Climatol.*, 34, 363, 367-373.
- Strzepek, K., G. Yohe, J. Neumann, and B. Boehlert (2010), Characterizing changes in drought risk for the United States from climate change, *Environmental Research Letters*, 5(4), 044012, doi:10.1088/1748-9326/5/4/044012.
- Sun, C., and S. Yang (2012), Persistent severe drought in southern China during winter-spring 2011: Large-scale circulation patterns and possible impacting factors, *Journal of Geophysical Research (Atmospheres)*, 117, 10112, doi:10.1029/2012JD017500.
- Svoboda, M. D., B. A. Fuchs, C. C. Poulsen, and J. R. Nothwehr (2015), The drought risk atlas: Enhancing decision support for drought risk management in the United States, *Journal of Hydrology*, 526, 274-286, doi:<https://doi.org/10.1016/j.jhydrol.2015.01.006>.
- Svoboda, M. D., M. Hayes, and D. Wood (2012), World Meteorological Organization, 2012: Standardized Precipitation Index User Guide, (*WMO-No. 1090*), Geneva.
- Tannehill, I. R. (1947), *Drought its causes and effects*, Princeton University Press, Princeton.
- Taylor, I. H., E. Burke, L. McColl, P. D. Falloon, G. R. Harris, and D. McNeall (2013), The impact of climate mitigation on projections of future drought, *Hydrol. Earth Syst. Sci.*, 17(6), 2339-2358, doi:10.5194/hess-17-2339-2013.

Taylor, I. H., E. Burke, L. McColl, P. D. Falloon, G. R. Harris, and D. McNeall (2012a), Contributions to uncertainty in projections of future drought under climate change scenarios, *Hydrology and Earth System Sciences Discussions*, 9, 12613-12653, doi:10.5194/hessd-9-12613-2012.

Taylor, K. E., R. J. Stouffer, and G. A. Meehl (2012b), An Overview of CMIP5 and the experiment design., *Bull. Amer. Meteor. Soc.*, (doi:10.1175/BAMS-D-11-00094.1), 93, 485-498.

Thornthwaite, C. W. (1948), An Approach toward a Rational Classification of Climate, *Geographical Review*, 38(1), 55-94, doi:10.2307/210739.

van Vuuren, D. P., et al. (2011), The representative concentration pathways: an overview, *Climatic Change*, 109(1), 5, doi:10.1007/s10584-011-0148-z.

Varouchakis, E., and G. Corzo (2019), *Spatiotemporal Analysis of Extreme Hydrological Events* (<https://www.sciencedirect.com/book/9780128116890/spatiotemporal-analysis-of-extreme-hydrological-events>), doi:10.1016/C2016-0-01750-3.

Vicente-Serrano, S. M., S. Beguería, and J. I. López-Moreno (2009), A Multiscalar Drought Index Sensitive to Global Warming: The Standardized Precipitation Evapotranspiration Index, *Journal of Climate*, 23(7), 1696-1718, doi:10.1175/2009JCLI2909.1.

Vidal, J. P., E. Martin, L. Franchistéguy, F. Habets, J. M. Soubeyroux, M. Blanchard, and M. Baillon (2010), Multilevel and multiscale drought reanalysis over France with the Safran-Isba-Modcou hydrometeorological suite, *Hydrol. Earth Syst. Sci.*, 14(3), 459-478, doi:10.5194/hess-14-459-2010.

Weigel, K., et al. (2019), ESMValTool (v2.0) – Diagnostics for extreme events, regional model and impact evaluation and analysis of Earth system models in CMIP., *Geosci. Model Dev. Discuss.*, in prep.

Wilhite, D. A. (2000), Drought : a global assessment. Vol I and II Vol I and II.

Zotarelli (2013), Step by Step Calculation of the Penman-Monteith Evapotranspiration (FAO-56 Method).

APPENDIX

This appendix shows additional figures (figures A1-A4) that are discussed in this thesis.

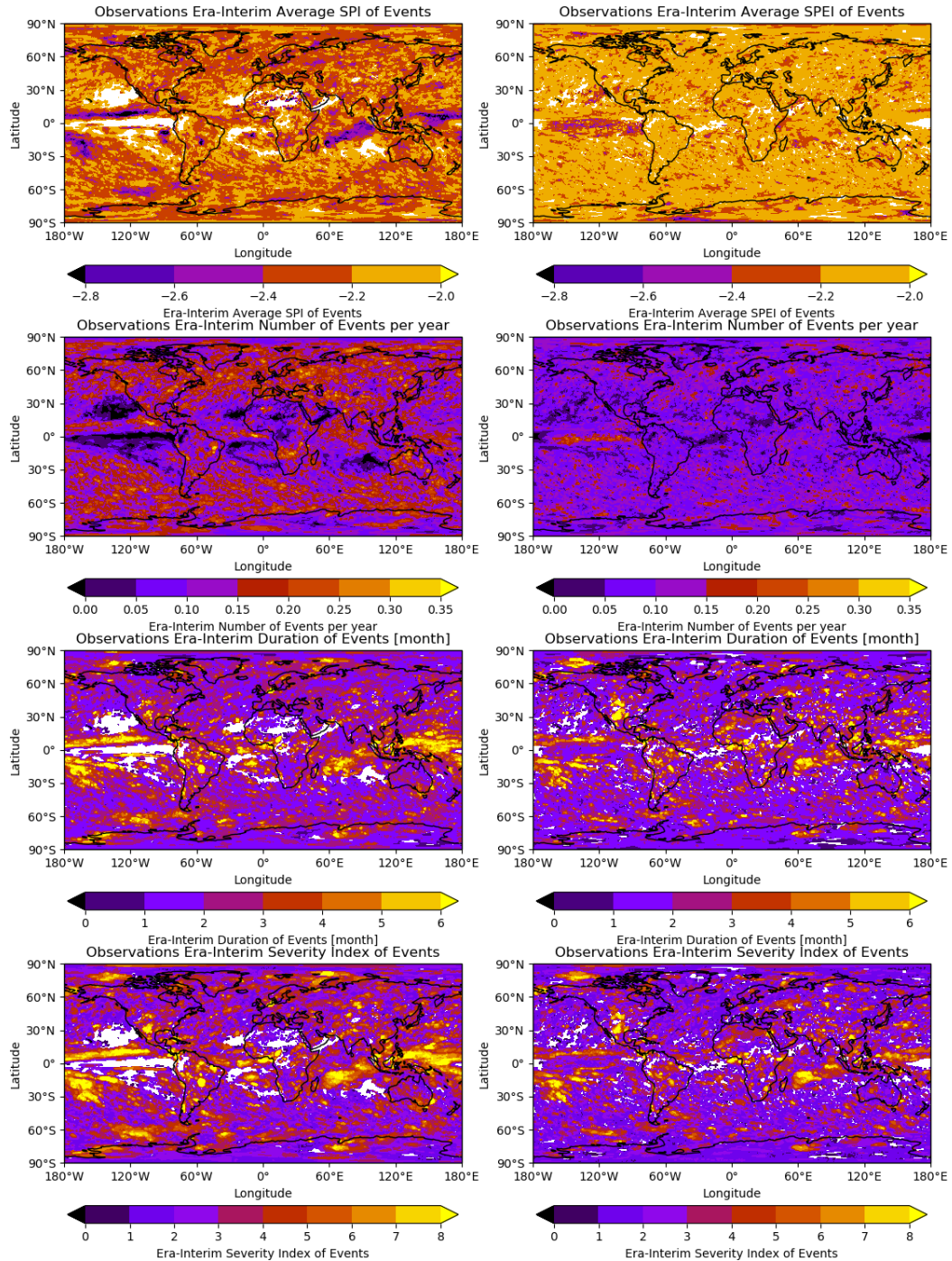


Figure A1: ERA-INTERIM (1979 to 2014) using SPI (left) and SPEI-PM (right) showing drought event characteristics of average SPI/SPEI, frequency, duration, and severity index from top to bottom, respectively. Produced using the ESMValTool, version 2.0a1, recipe_drought_events.yml and recipe_drought_events_obs_speipen_cmip6_2.yml.

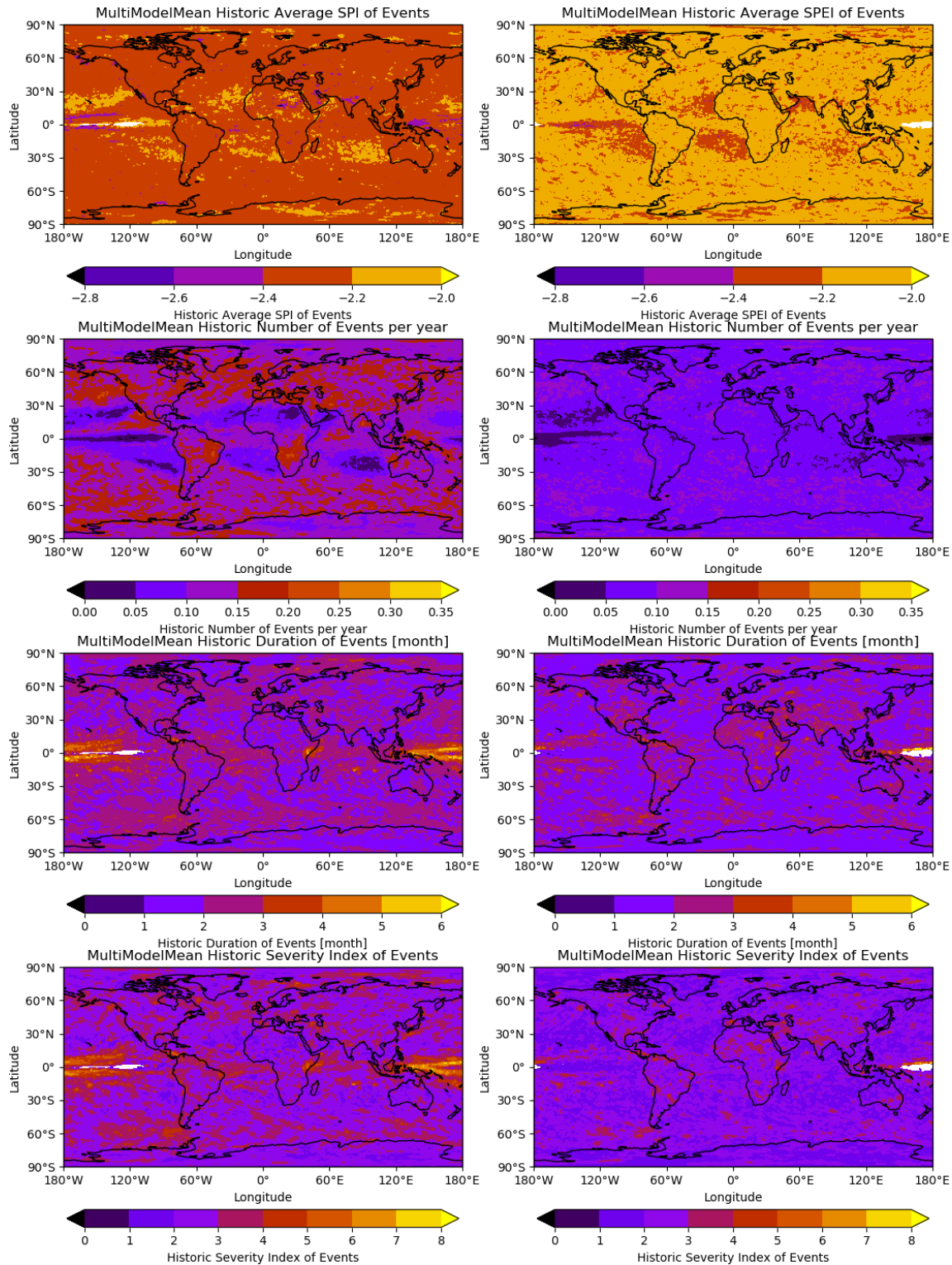


Figure A2: 7 CMIP6 multi-model mean historic scenario runs (1979 to 2014) using SPI (left) and SPEI-PM (right) showing drought event characteristics of average SPPI/SPEI, frequency, duration, and severity index from top to bottom, respectively. Produced using the ESMValTool, version 2.0a1, recipe_drought_events.yml.

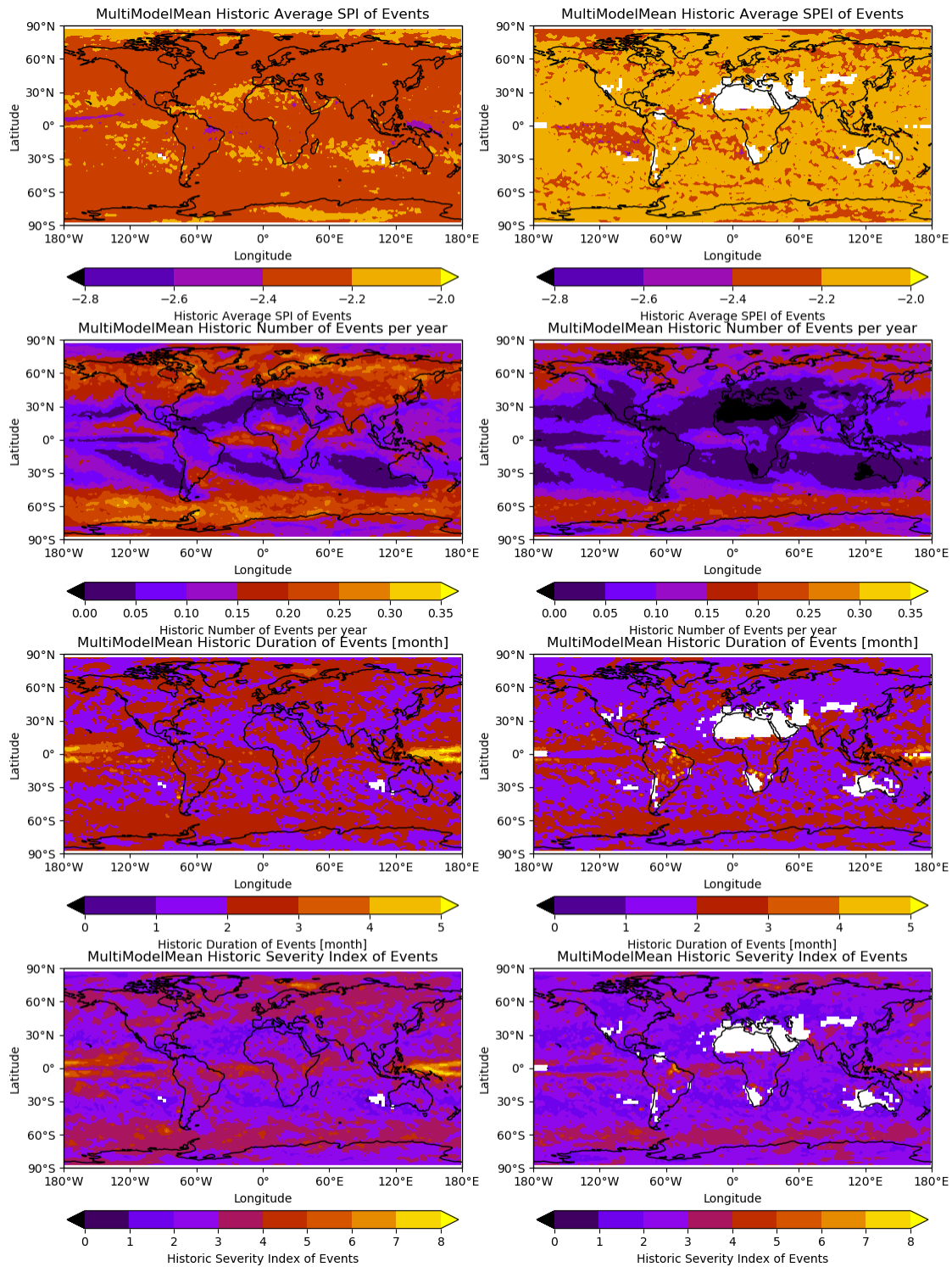


Figure A3: 7 CMIP6 multi-model mean historical runs (1950 to 2000) using SPI (left) and SPEI-PM (right) showing drought event characteristics of average SPI/SPEI, frequency, duration, and severity index from top to bottom, respectively. Produced using the ESMValTool, version 2.0a1, recipe_drought_events.yml.

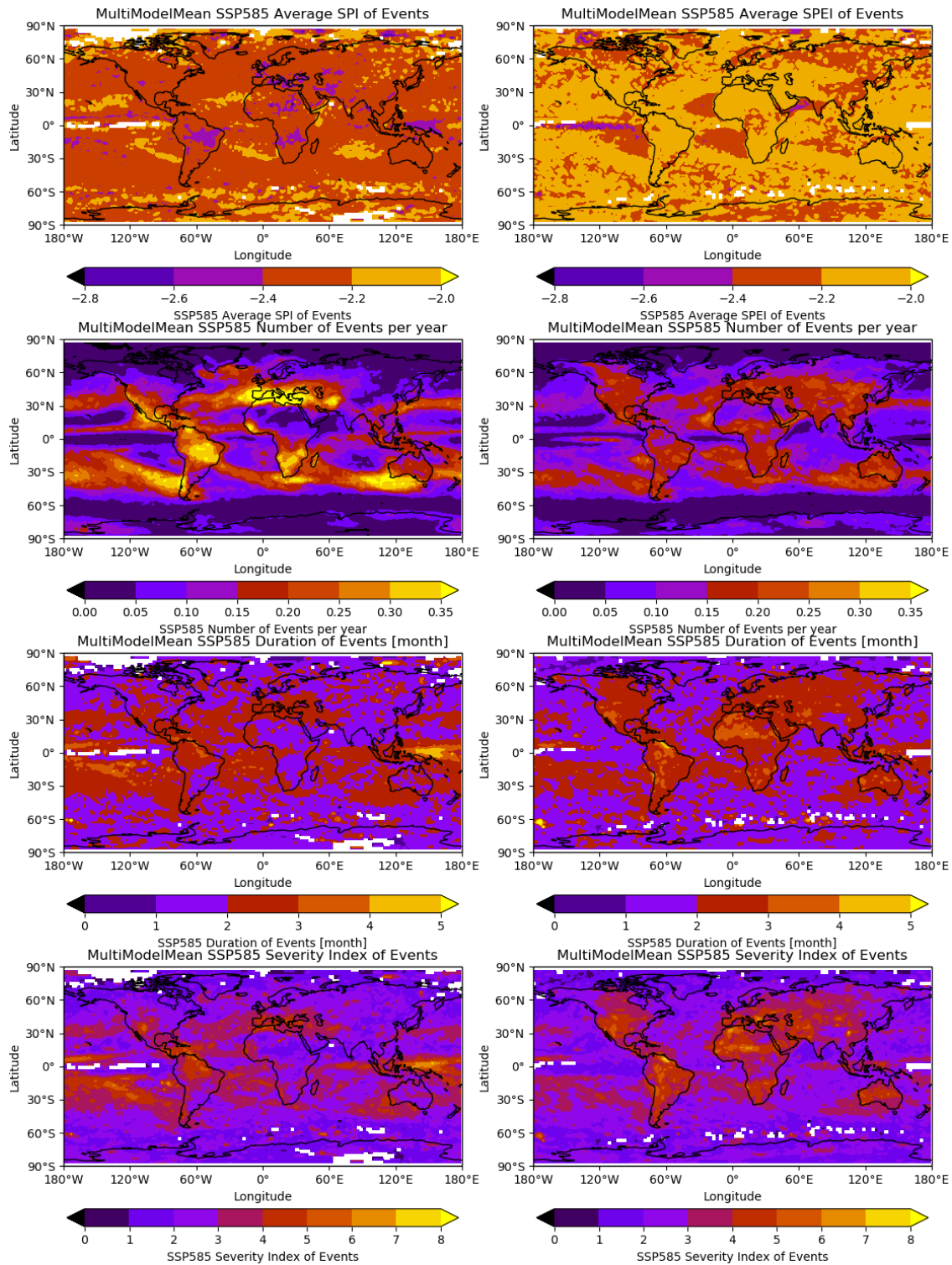


Figure A4: 7 CMIP6 multi-model mean SSP5-85 scenario runs (2050 to 2100) using SPI (left) and SPEI-PM (right) showing drought event characteristics of average SPI/SPEI, frequency, duration, and severity index from top to bottom, respectively. Produced using the ESMValTool, version 2.0a1, recipe_drought_events.yml.

ACKNOWLEDGEMENTS

I would like to thank Prof. Dr. Veronika Eyring, as my scientific supervisor and first evaluator, for giving me the possibility to write my Master thesis in her group at the Department of Climate Modelling. I appreciate her great support and helpful mentoring during my thesis. I would also like to thank her for giving me the opportunity to be a part of some scientific workshops, trainings, Hiwi job, meeting other great scientists and even being a part of an upcoming literature.

I also would like to thank Prof. Dr. Markus Reichstein for being my second evaluator. I appreciate his inputs and critics that drove this work to this present stage. I would like to say thank you for his availability despite his tight schedule to support the completion of this work.

A special thanks goes to Dr. Katja Weigel for her technical support with MISTRAL, ESMValTool, and especially for taking me through the basics of LINUX programming and for the helpful discussions and proof readings. I would like to thank Bettina Gier for the helpful discussions, github understanding, proof reading and scientific feedback on this work. I appreciate the entire Earth System Model Evaluation Group, under the lead of Prof. Dr Veronika Eyring, for the constant improvement of the ESMValTool software.

A very special thanks goes to my fiancé, Babajide Adeyemo, for his every time support, morally and financially throughout my Master study. I also thank my family and friends, for keeping me grounded and relieving me from worries many times when I feel exhausted.

DECLARATION OF HONOUR

Name:

Matriculation No:

.....

.....

I hereby confirm on my honor that I personally prepared the present academic work and carried out myself the activities directly involved with it. I also confirm that I have used no resources other than those declared. All formulations and concepts adopted literally or in their essential content from printed, unprinted or internet sources have been cited according to the rules for academic work and identified by means of footnotes or other precise indications of source.

The support provided during the work, including significant assistance from my supervisor has been indicated in full.

The academic work has not been submitted to any other examination office authority. The work is submitted in printed and electronic form. I confirm that the content of the digital version is completely identical to that of the printed version.

Date:

Signature:

.....

.....

Declaration of publication

- I hereby agree that my thesis will be available for third party review for the purpose of academic research.

Date

Signature

.....

.....